Time-Reversal Wireless Paradigm for Green Internet of Things: An Overview

Yan Chen, *Member*, *IEEE*, Feng Han, *Member*, *IEEE*, Yu-Han Yang, *Student Member*, *IEEE*, Hang Ma, Yi Han, Chunxiao Jiang, *Member*, *IEEE*, Hung-Quoc Lai, *Member*, *IEEE*, David Claffey, Zoltan Safar, and K. J. Ray Liu, *Fellow*, *IEEE*

***Abstract*—In this paper, we present an overview of the time-reversal (TR) wireless paradigm for green Internet of Things (IoT). It is shown that the TR technique is a promising technique that focuses signal waves in both time and space domains. The unique asymmetric architecture significantly reduces the cost of the terminal devices, the total number of which is expected to be very large for IoT. The focusing effect of the TR technique can harvest the energy of all the multi-paths at the receiver, which improves the energy efficiency of the wireless transmission and thus the battery life of terminal devices in IoT. Facilitated by the high-resolution spatial focusing, the TR division multiple access scheme leverages the uniqueness of the multi-path profiles in the rich-scattering environment and maps them into location-specific signatures, so that spatial multiplexing can be achieved for multiple users operating on the same spectrum. In addition, the TR system can easily support heterogeneous terminal devices by providing various quality-of-service (QoS) options through adjusting the waveform and rate backoff factor. Finally, the unique location-specific signature in TR system can provide additional physical-layer security and thus can enhance the privacy and security of customers in IoT. All the advantages show that the TR technique is a promising paradigm for IoT.**

***Index Terms*—Internet of Things (IoT), spatial focusing, temporal focusing, time reversal (TR), time-reversal division multiple access (TRDMA).**

I. Introduction

DURING the past decade, the *Internet of Things* (IoT) has drawn great attention from both academia and industry, since it offers challenging notion of creating a world where all the *things*, known as smart objects [1], around us are connected, typically in a wireless manner, to the Internet and communicate with each other with minimum human intervention [2]–[4]. An example of IoT system is shown in Fig. 1. The ultimate goal of IoT is to create a better world where things around us know what we like, what we want, and what we need and act accordingly without explicit instructions [5], and thus improve the quality of our lives and consistently reduce the ecological impact of mankind on the planet [6].

The term "IoT" was first proposed by Kevin Ashton in his presentation at Procter&Gamble (P&G) in 1999 [7]. During the presentation, Ashton envisioned the potential of IoT by stating "The Internet of Things has the potential to change the world, just as the Internet did. Maybe even more so." Such a concept then became popular when the MIT Auto-ID center presented their vision of IoT in 2001 [8]. In 2005, IoT was formally introduced by the International Telecommunication Union (ITU) through the ITU Internet report [9].

With a very broad vision, IoT has shown its great potential to improve the quality of our lives. However, the research into the IoT is still in its infancy and there are still a lot of challenges needed to be addressed before the realization of IoT. In the following, we summarize some key technical challenges from the perspective of wireless communication, which is the essential technology of IoT to allow people and things to connect to Internet anywhere at anytime [10]

1) *Better battery life*: Typically the things in IoT are powered with small batteries, due to which the power consumption is low and thus requires low computational complexity of the wireless communication techniques.
2) *Multiple active things*: The IoT is expected to have many concurrent active things transmitting data, which leads to severe interference among things. Thus, low interference wireless technologies are desired.
3) *Low-cost terminal devices*: For widespread adoption of the IoT technology, the cost at the terminal devices, i.e., things, needs to be low. Therefore, simple processing at the terminal devices' side is preferred.
4) *Heterogeneous terminal devices*: Different from current wireless systems that have a collection of rather uniform devices, it is to be expected that the IoT will exhibit a much higher level of heterogeneity, as things that are totally different in terms of functionality, technology and application fields will belong to the same communication environment. Thus, the wireless solution to IoT should be able to support heterogeneous terminal devices with

Manuscript received October 30, 2013; revised January 28, 2014; accepted February 11, 2014. Date of publication February 27, 2014; date of current version May 05, 2014.

Y. Chen, Y.-H. Yang, H. Ma, Y. Han, Z. Safar, and K. J. Ray Liu are with Origin Wireless Communications Inc., College Park, MD 20742 USA, and also with the Department of Electrical and Computer Engineering, University of Maryland, College Park, MD 20742 USA (e-mail: yan@umd.edu; yhyang@umd.edu; hangma@umd.edu; yhan1990@umd.edu; zsafar@umd.edu; kjrliu@umd.edu).

F. Han was with the Department of Electrical and Computer Engineering, University of Maryland, MD 20742 USA, and with Origin Wireless Communications Inc., College Park, MD 20742 USA. He is now with Qualcomm Inc., San Diego, CA 92121 USA (e-mail: hanf@ieee.org).

C. Jiang was with the Department of Electrical and Computer Engineering, University of Maryland, MD 20742 USA, and with Origin Wireless Communications Inc., College Park, MD 20742 USA. He is now with the Department of Electronic Engineering, Tsinghua University, Beijing 100084, China (e-mail: chx.jiang@gmail.com).

H.-Q. Lai and D. Claffey are with Origin Wireless Communications Inc., College Park, MD 20742 USA (e-mail: quoc.lai@originwirelesscomm.com; david.claffey@originwirelesscomm.com).

Color versions of one or more of the figures in this paper are available online at http://ieeexplore.ieee.org.

Digital Object Identifier 10.1109/JIOT.2014.2308838

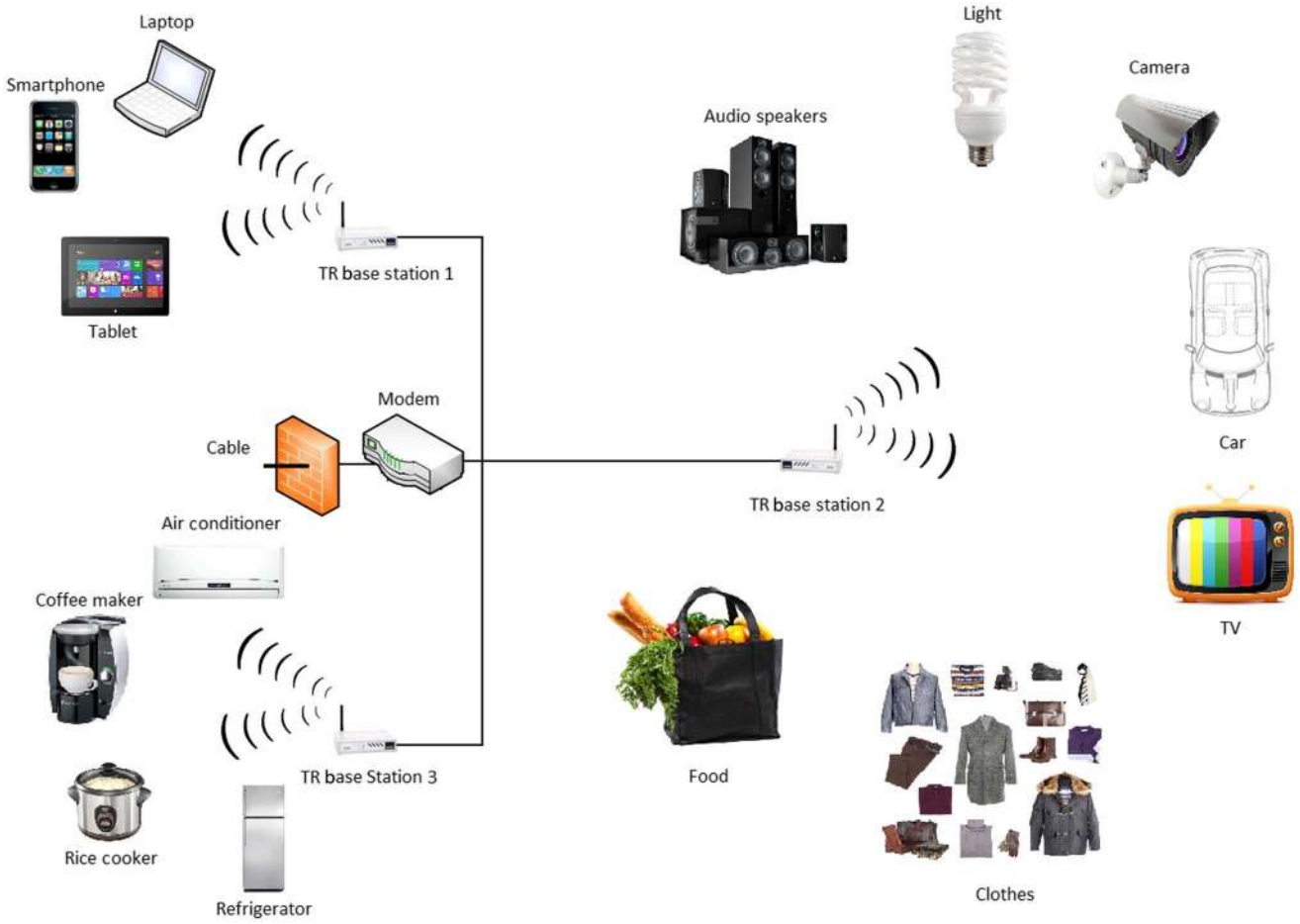

Fig. 1. Illustration of TR system for IoT.

different quality-of-service (QoS) options such as from very low bit rate to very high.

5) *Scalability*: The density of the things in IoT may be very high or low, which requires the wireless technology to be highly scalable to provide satisfactory QoS for low to high density areas.
6) *Privacy and security*: Since every thing in IoT has a unique identification, there is a need to have a technically sound solution to guarantee privacy and the security of the customers in order to have a widespread adoption of IoT.

To qualify as a good wireless communication solution to IoT, a technology should be able to handle the challenges raised above. Currently existing wireless technologies for IoT can be classified into two groups: 1) wireless technologies for low-data-rate and low-power applications such as remote control [11], [12]; and 2) wireless technologies for high-data-rate applications such as video streaming [13]–[17]. Note that the technologies suitable for low-data-rate applications may not be able to meet the requirements of the high-data-rate applications.

A typical wireless communication technology suitable for low power, low-data-rate applications is ZigBee [11]. Mainly based on IEEE 802.15.4, ZigBee can operate in the 868 MHz, 915 MHz, and 2.4 GHz bands with respective data rates of 20, 40, and 250 kb/s. A similar technology is Z-Wave [12], whose main purpose is to enable short message transmission from a control node to multiple nodes. The maximum speed of Z-Wave is 200 kb/s working at 2.4-GHz band. The most significant advantage of ZigBee and Z-Wave is the low price [18], [19]. For instance, there exist $\$3-\$5$ chips including RF module, the digital baseband module, and a programmable microcontroller. Both of these technologies were designed for low-power applications in battery-operated devices. Moreover, ZigBee even includes a sleep-mode mechanism to reduce power consumption. The complexity of hardware is quite low: 32–128 kbytes of memory is enough to implement the system including the higher layers. On the other hand, the most obvious disadvantage of ZigBee and Z-Wave is their low data rate. Moreover, the 2.4-GHz frequency band is already crowded with interfering devices, e.g., microwave ovens, WiFi equipment, and cordless phones. The sub-GHz electromagnetic (EM) waves propagate very far, so very high node density may not be achievable due to the high interference levels created by other similar devices.

The most popular technologies for high-data-rate applications are Bluetooth [13] and WiFi [14]. Bluetooth, based on IEEE 802.15.1, is a wireless technology for exchanging data over short distance. Compared with ZigBee and Z-Wave, the data rate could be increased to megabit per second (Mbps). WiFi, based on IEEE 802.11, is a popular technology that allows an electronic device to exchange data or connect to the Internet wirelessly. The speed of WiFi can achieve up to several gigabit per second (Gbps) according to IEEE 802.11ac with the help of MIMO and very high-order modulation. The most important advantage of these

two technologies is the high data rate. However, they require higher power consumption, higher complexity of hardware (MIMO in WiFi) and thus higher price [20]. Since both transmitter and receiver use the same architecture, i.e., symmetric architecture is used, the power consumption of terminal devices is high. In addition, a large number of WiFi access points (APs) deployed close to each other operating in the same or adjacent channels will severely interfere with each other. Thus, these technologies do not seem to offer robust performance in interference-limited scenarios even with costly terminal devices. Another possible technology is the 3G/4G mobile communications [21]–[23]. However, the poor indoor coverage of 3G/4G signals greatly limit its application to IoT, where communications mostly happen in indoor environment.

From the above discussions, we can see that existing technologies can only address partial challenges while leaving the rest unaddressed, e.g., both the heterogeneity and scalability challenges cannot be handled by existing technologies. A natural question to ask is: is there a wireless communication technique that can address most, if not all, challenges? As pointed out in [24], time-reversal (TR) signal transmission is an ideal paradigm for low-complexity, low energy consumption green wireless communication because of its inherent nature to fully harvest energy from the surrounding environment by exploiting the multi-path propagation to recollect all the signal energy that could be collected as the ideal RAKE receiver. The theoretic analysis in [24] shows that a typical TR system has a potential of over an order of magnitude of reduction in power consumption and interference alleviation, which means that TR system can provide better battery life and support multiple concurrent active users. Moreover, with our proposed asymmetric TR architecture, only one-tap detection is needed at the receiver side [25], thus the computational complexity at the terminal devices is low, which means the cost of the terminal devices is also low. Note that the achievable rate can still be very high when the bandwidth is wide enough as shown in [26]. In addition, the TR system can easily support heterogeneous terminal devices by providing various QoS options through adjusting the waveform and backoff factor [25], [27]. Finally, the unique location-specific signature in TR system can provide additional physical-layer security and thus can enhance the privacy and security of customers in IoT [24]. Overall, we will provide an overview to show that TR technique is an ideal paradigm for IoT.

The rest of the paper is organized as follows. In Section II, we introduce some basic concepts of TR technique. Then, we propose in Section III an asymmetric TR division multiple access (TRDMA) architecture and discuss in details why TR is an ideal paradigm for IoT. In Section IV, we discuss other challenging issues and future directions including advanced waveform design, MAC layer issues, and low-cost high-speed analog-to-digital converter (ADC) and DAC. Finally, we draw conclusions in Section V.

II. Some Basics of TR

A. The Basic Principles of TR

The TR signal processing is a technology to focus the power of signal waves in both time and space domains. The research of TR can date back to early 1970s, when phase conjugation was first observed and studied by Zeldovich *et al.* [28]. Unlike the phase conjugation that uses an holographic or parametric pumping [29], the TR uses transducers to record the signal waves and enables signal processing on the recorded waveforms.

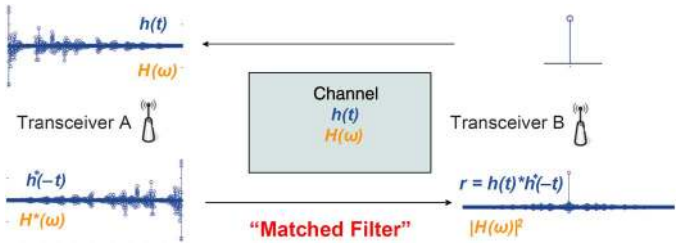

Fig. 2. Time reversal signal processing principle.

The TR signal processing was applied by Fink *et al.* in 1989 [30], followed by a series of theoretical and experimental works in acoustic communications [31]–[38]. As found in acoustic physics [30]–[34] and then further validated in practical underwater propagation environments [35]–[37], the energy of the TR acoustic waves from transmitters could be refocused only at the intended location with very high spatial resolution. Since TR can make full use of multi-path propagation and also requires no complicated channel processing and equalization, it was later verified and tested in wireless radio communication systems. Experimental validations of TR technique with EM waves have been conducted in [24], [39]–[45], including the demonstration of spatial and temporal focusing properties [24], [39]–[45] and channel reciprocity [24], [41]. The feasibility of applying TR technique into ultra-wideband (UWB) communications has been studied in [46]–[48] with the focus on the bit error rate (BER) performance through simulation. A system-level theoretical investigation and comprehensive performance analysis of a TR-based multiuser communication system was conducted in [25], where the concept of TRDMA was proposed. To improve the performance of the TRDMA systems, interference suppression through waveform design [27], [49] and interference cancelation [50] are proposed. The implementation complexity issue is studied in [26], [51], and [52]. Moreover, as shown in [53], [54], with random scatterers, TR can achieve focusing that is far beyond the diffraction limit, i.e., half wavelength.

The principle of TR transmission is very simple, as demonstrated in Fig. 2. In this figure, when transceiver A wants to transmit information to transceiver B, transceiver B first has to send an impulse-like pilot signal that propagates through a scattering and multi-path environment and the resulting waveforms are received and recorded by transceiver A. This is called channel probing phase. After that, transceiver A simply time-reverses (and conjugated, if the signal is complex valued) the received waveform and then transmits it back through the same channel to transceiver B. This is called TR-transmission phase.

There are two basic assumptions for the TR communication system to work.

1) Channel reciprocity: the impulse responses of the forward link channel and the backward link channel are assumed to be identical.
2) Channel stationarity: the channel impulse responses (CIRs) are assumed to be stationary for at least one probing-and-transmitting cycle.

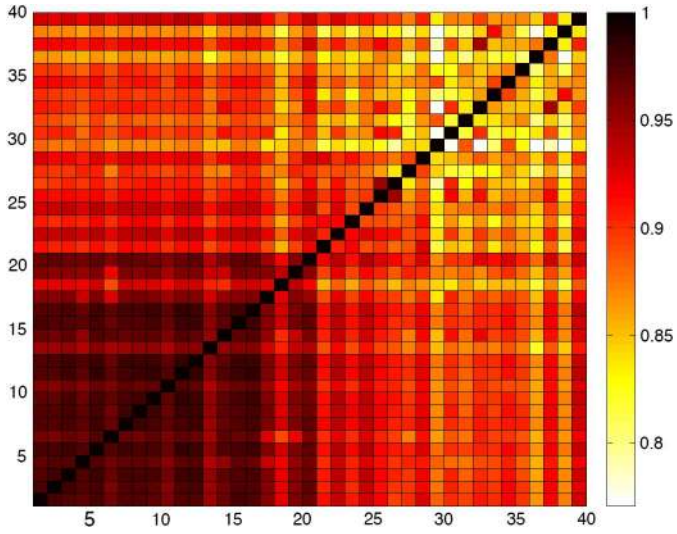

Fig. 3. Correlation of channel responses at different time epochs [24].

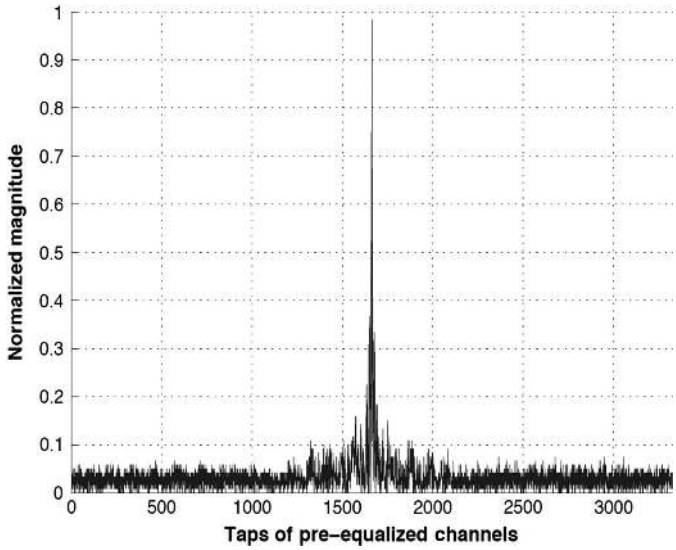

Fig. 4. Temporal focusing effect obtained from experiments [24].

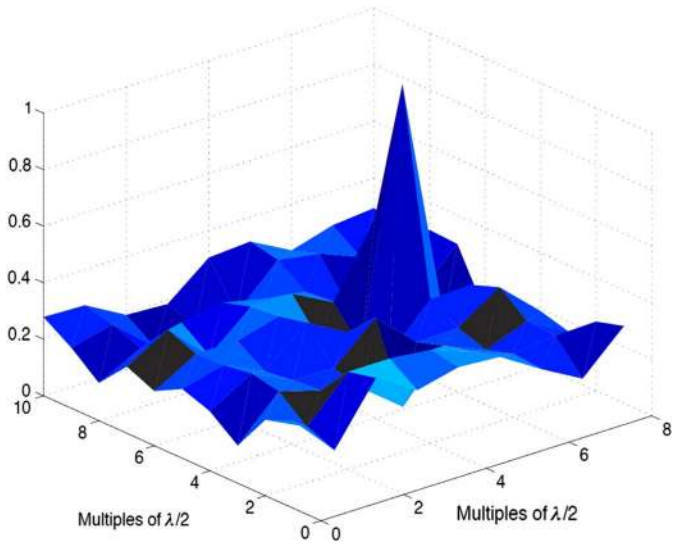

Fig. 5. Spatial focusing effect obtained from experiments [24].

These two assumptions generally hold in reality, especially for indoor environment, as validated through real experiments in [55] and [24]. In [55], Qiu *et al.* conducted experiments in a campus lab area and showed that the correlation between the impulse response of the forward link channel and that of backward link channel is as high as about 0.98, which means that the channel is highly reciprocal. In [24], Wang *et al.* showed with experimental results that the multi-path channel of an office environment is actually not changing a lot. In their experiment, Want *et al.* measured the channel information every one minute, and a total of 40 channel snapshots were taken and stored, where the first 20 snapshots correspond to a static environment, snapshots 21 to 30 correspond to a moderately varying environment, and snapshots 31 to 40 correspond to a varying environment. The experimental results are shown in Fig. 3, where we can see that most the correlation coefficients between different snapshots are higher than 0.8 and those between static snapshots are above 0.95, which means that the channel is highly stationary.

By utilizing channel reciprocity, the re-emitted TR waves can retrace the incoming paths, ending up with a constructive sum of signals of all the paths at the intended location and a "spiky" signal-power distribution over the space, as commonly referred to as *spatial focusing effect*. Also from the signal processing point of view, in the point-to-point communications, TR essentially leverages the multi-path channel as a matched filter and focuses the wave in the time domain as well, as commonly referred as *temporal focusing effect*. By treating the environment as a facilitating matched filter computing machine, the complexity of TR systems is significantly reduced, which is ideal for IoT applications as we will discuss later.

B. Temporal Focusing and Spatial Focusing of TR

In principle, the mechanisms of reflection, diffraction, and scattering in wireless medium give rise to the uniqueness and independence of the CIR of each multi-path communication link [56]. Obtained from real indoor experiments [24], Figs. 4 and 5 show that, when the re-emitted TR waves from transceiver A propagate in the wireless medium, the location of transceiver B is the only location that is associated with the reciprocal CIR. That is to say that given the re-emitted TR waveform from transceiver A that is specific to the CIR between transceivers A and B, the environment will serve as a natural matched filter only for the intended transceiver B. As a result, the temporal focusing effect of the specific re-emitted TR waveform can be observed only at the location of transceiver B. It means that at the time instance of time focusing, the signal power not only exhibits a strong peak in the time domain at transceiver B as shown in Fig. 4, but also concentrates spatially only at the location of transceiver B in the rich multi-path environments as shown in Fig. 5. A physical meaning is that at this moment, it creates a resonating effect due to the TR transmission.

Experimental results in both acoustic/ultrasound domain and radio frequency (RF) domain further verified the temporal focusing and spatial focusing effects of the TR transmission, as predicted by theory. Fink *et al.* [30]–[34] found that acoustic energy can be refocused on the source with very high resolution

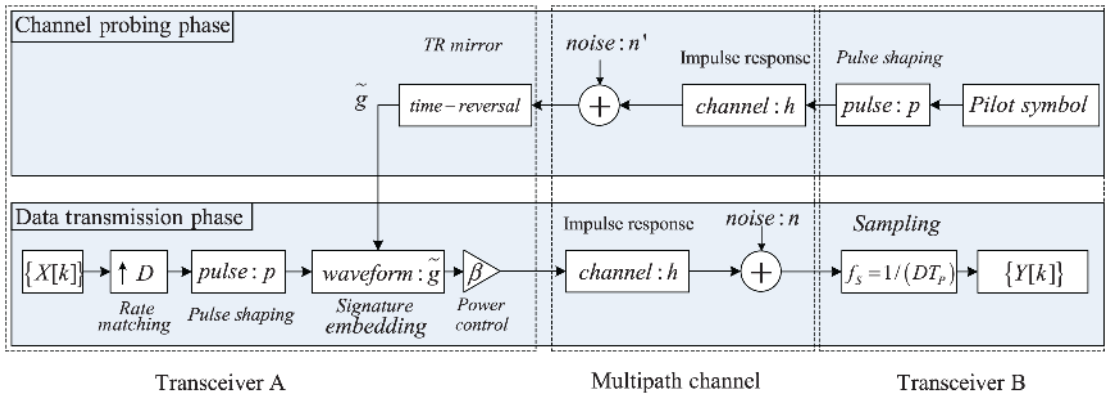

Fig. 6. Basic time reversal communications.

(wavelength level). In [35]–[37], acoustics experiments in the ocean were conducted to validate the focusing effects of TR in real underwater propagation environments. In the RF domain, experiments in [39], [40], and [46] demonstrated the spatial and temporal focusing properties of EM signal transmission with TR by taking measurements in RF communications. Furthermore, a TR-based interference canceler to mitigate the effect of clutter was presented in [57], and target detection in a highly cluttered environment using TR was investigated in [58] and [59]. In [24], real-life RF experiment results were obtained in typical indoor environments, which shows the great potential of TR as a new paradigm of the green wireless communications.

In the context of communication systems, the temporal focusing effect concentrates a large portion of the useful signal energy of each symbol within a short time interval, which effectively suppresses the inter-symbol interference (ISI) for high-speed broadband communications. The spatial focusing effect allows the signal energy to be harvested at the intended location and reduces leakage to other locations, leading to a reduced required transmit power consumption and lower co-channel interference to other locations. The benefits and unique advantages of TR-based communication systems due to the temporal and spatial focusing effects promise a great potential for the applications of IoT, as will be discussed in the remaining parts of this paper.

C. TR Communication System

A very simple TR-based communication system is shown in Fig. 6. The CIR between the two transceivers is modeled as

$$h(t) = \sum_{v=1}^{V} h_v \delta(t - \tau_v) \tag{1}$$

where h_v is the complex channel gain of the vth path of the CIR, and τ_v is the corresponding path delay, and the V is the total number of the underlying multi-paths (assuming infinite system bandwidth and time resolution). Without loss of generality, we assume that $\tau_1 = 0$ in the following discussion, i.e., the first path arrives at time $t = 0$, and as a result, the delay spread of the multi-path channel T is given by $T = \tau_V - \tau_1 = \tau_V$.

Constrained by the limited bandwidth of practical communication system, pulse shaping filters are typically used to limit the effective bandwidth of the transmission. Generally, the duration of the pulse T_P is limited by the available bandwidth B through the simple relation $T_P = 1/B$.

1) Channel Probing Phase: Prior to transceiver A's TR-transmission, transceiver B first sends out a pulse $p(t)$ of duration T_P (other than an ideal impulse which demands infinite bandwidth) which propagates to transceiver A through the multi-path channel $h(t)$, where transceiver A keeps a record of the received waveform $\tilde{h}(t)$, which is the convolution of $h(t)$ and $p(t)$, represented as follows:

$$\tilde{h}(t) = \int_{t-T_P}^{t} p(t-\tau)h(\tau)d\tau, \quad 0 \leqslant t \leqslant T + T_p \;\&\; T_P \ll T \tag{2}$$

where $\tilde{h}(t)$ can be treated as an equivalent channel response for the system with a limited bandwidth B. From (2), one can see that for those paths whose time differences are less than the pulse duration T_P, they are mixed together due to the limited system bandwidth B. Also for $|t_1 - t_2| > T_P$, the received values $\tilde{h}(t_1)$ and $\tilde{h}(t_2)$ are determined by completely different sets of paths. Therefore, given a limited bandwidth B, the corresponding pulse duration T_P determines the time-domain resolution to resolve two adjacent paths. In other words, from the system's perspective, those paths whose time differences are within the duration T_P are treated like one path in the equivalent channel response $\tilde{h}(t)$.

2) Data Transmission Phase: Upon receiving the waveform, transceiver A time-reverses (and conjugate, when complex-valued) the received waveform $\tilde{h}(t)$, and uses the normalized TR waveform as a basic signature waveform $\{\tilde{g}(t)\}$, i.e.,

$$\tilde{g}(t) = \frac{\tilde{h}^*(-t)}{\sqrt{\int_0^{T+T_P} |\tilde{h}(\tau)|^2 d\tau}} = \frac{\int_t^{t+T_P} p^*(-t+\tau)h^*(-\tau)d\tau}{\sqrt{\int_0^{T+T_P} |\tilde{h}(\tau)|^2 d\tau}}. \tag{3}$$

Defining $g(t) \triangleq h^*(-t)$ and $q(t) \triangleq p^*(-t)$, $\tilde{g}(t)$ in (3) can be represented as

$$\tilde{g}(t) = (g * q)(t). \tag{4}$$

At transceiver A, there is a sequence of information symbols $\{X[k]\}$ to be transmitted to transceiver B. Typically,

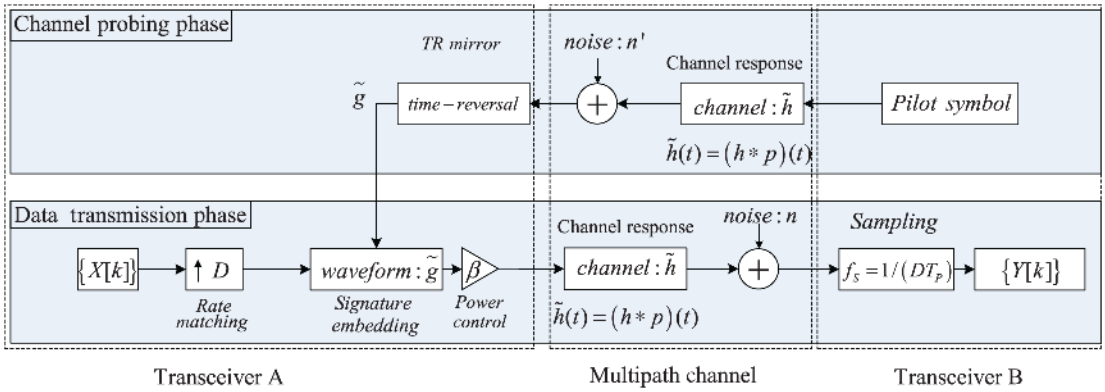

Fig. 7. Basic TR communications with equivalent channel response $\tilde{h}(t)$.

the symbol rate can be much lower than the system chip rate.[1] Therefore, a rate backoff factor D is introduced to match the symbol rate with the chip rate by inserting $(D-1)$ zeros between two symbols [24], [25], [46], [60]. Applying the pulse shaping filter $p(t)$,

$$W(t) = \sum_{k\in\mathbb{Z}^+} X[k]\cdot p(t-kDT_P) \tag{5}$$

and the transmitted signal[2] can be expressed as

$$S(t) = \beta(W*\tilde{g})(t) = \beta\sum_{k\in\mathbb{Z}^+} X[k](p*q*g)(t-kDT_P). \tag{6}$$

The signal received at transceiver B is the convolution of $S(t)$ and $h(t)$, plus additive white Gaussian noise (AWGN) $\tilde{n}(t)$ with zero-mean and variance σ_N^2, i.e.,

$$\begin{aligned} Y(t) &= (S*h)(t)+\tilde{n}(t)\\ &= \tilde{n}(t)+\beta\sum_{k\in\mathbb{Z}^+} X[k](p*q*g*h)(t-kDT_P)\\ &= \tilde{n}(t)+\beta\sum_{k\in\mathbb{Z}^+} X[k](\tilde{h}*\tilde{g})(t-kDT_P) \end{aligned} \tag{7}$$

where $\tilde{h}(t) = (p*h)(t)$ and $\tilde{g}(t) = (q*g)(t)$.

Thanks to the temporal focusing, when $t = kDT_P$, the power of $(\tilde{h}*\tilde{g})(t-kDT_P)$ achieves its maximum for $X[k]$, i.e.,

$$(\tilde{h}*\tilde{g})(0) = \int_0^{T+T_P}\tilde{h}(\tau)\tilde{g}(-\tau)d\tau = \sqrt{\int_0^{T+T_P}|\tilde{h}(\tau)|^2 d\tau}. \tag{8}$$

As the receiver, transceiver B simply samples the received signal every DT_P seconds at $t = kDT_P$,[3] for $k = 1, 2, \ldots$, in order to detect the symbol $X[k]$

$$\begin{aligned} Y[k] &= Y(t{=}kDT_P)\\ &= \beta\sum_{l=-\left\lfloor\frac{T+T_P}{DT_P}\right\rfloor}^{\left\lfloor\frac{T+T_P}{DT_P}\right\rfloor} X[k{+}l](\tilde{g}{*}\tilde{h})(lDT_P){+}\tilde{n}(kDT_P)\\ &= \underbrace{\beta(\tilde{h}{*}\tilde{g})(0)X[k]}_{\text{Signal}}+\underbrace{\beta\sum_{\substack{l=-\left\lfloor\frac{T+T_P}{DT_P}\right\rfloor\\ i\neq 0}}^{\left\lfloor\frac{T+T_P}{DT_P}\right\rfloor} X[k{+}l](\tilde{g}{*}\tilde{h})(lDT_P)}_{\text{ISI}}+\underbrace{n[k]}_{\text{Noise}}, \end{aligned} \tag{9}$$

where $n[k] \triangleq \tilde{n}(kDT_P)$.

Consequently, the resulting signal-to-interference-plus-noise ratio (SINR) is obtained as

$$\text{SINR} = \frac{\beta^2\int_0^{T+T_P}|\tilde{h}(\tau)|^2 d\tau}{\beta^2\sum_{\substack{l=-\left\lfloor\frac{T+T_P}{DT_P}\right\rfloor\\ l\neq 0}}^{\left\lfloor\frac{T+T_P}{DT_P}\right\rfloor}|(\tilde{g}*\tilde{h})(lDT_P)|^2+\sigma_N^2} \tag{10}$$

assuming that each information symbol $X[k]$ has unit power.

3) An Equivalent System Model with Limited Bandwidth: Based on (2)–(10), one can come up with an equivalent system model shown in Fig. 7 for the system with limited system bandwidth as shown in Fig. 6. In the equivalent system model, $\tilde{h}(t) = (h*p)(t)$ is treated as the effective channel response for such a finite-bandwidth system, taking into account the use of the band-limiting pulse shaping filter $p(t)$. Accordingly, the time-reversed (and conjugated) version of the equivalent channel response $\tilde{g}(t) = \tilde{h}^*(-t)$ is the corresponding TR signature waveform for the equivalent model.

[1]The duration of each chip is T_P.

[2]Note that in this paper, the base-band system model is considered. As a result, no RF components are included in the system diagrams.

[3]It is assumed here that the synchronization has been achieved at a reference time $t = 0$, without loss of generality.

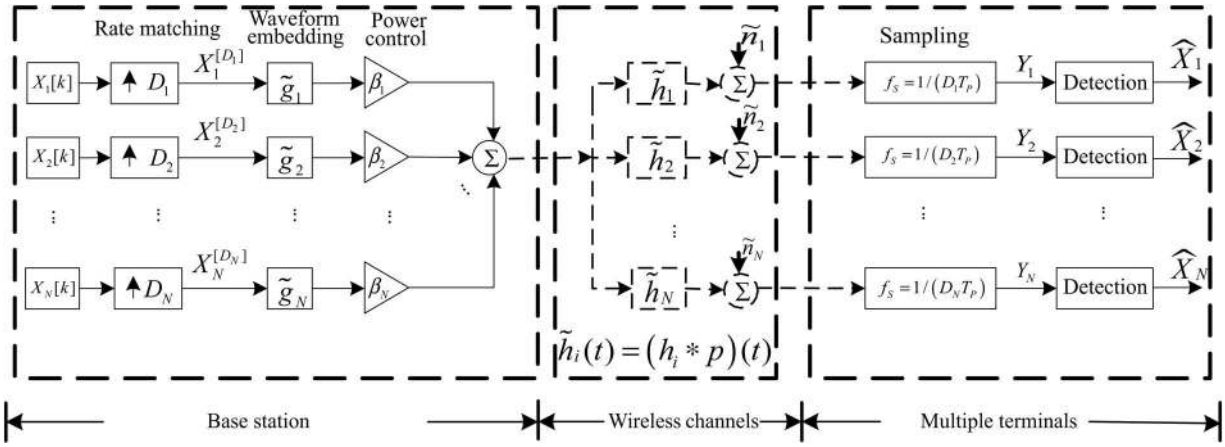

Fig. 8. Basic diagram of the TRDMA downlink.

In the following discussion of the TRDMA scheme in this paper, we use the simpler equivalent model by looking at the effective channel response $\tilde{h}(t) = (h * p)(t)$, which can be verified by comparing Figs. 6 and 7.

III. Asymmetric TRDMA Architecture for IoT

Based on TR technique, we recently introduced in [25] a novel multi-user media access scheme, TRDMA, for wideband communication. Leveraging the unique temporal and spatial focusing effects of the TR technique [24], [61], the TRDMA exploits the spatial degrees of freedom of the environment and uses the multipath channel profile associated with each user's location as a location-specific signature for the user. Moreover, such channel profiles may be further improved by mixing spatial degrees of freedom and temporal degrees of freedom as shown in [62] and [63].

With the concept of TRDMA, in this section, we propose an asymmetric TRDMA architecture for IoT, where most of the computational complexities are concentrated at the more powerful base station (BS), resulting in a minimal complexity and cost at the terminal devices in both uplink and downlink. As shown in Fig. 1, the proposed IoT system consists of multiple TR BSs and each BS serves multiple heterogeneous terminal devices, which ranges from laptop and TV to light and clothes. In the following, we will first focus on the single BS scenario and then discuss the multiple-BS scenario in Section III-E.

A. Channel Probing Phase

Consider a wireless broadband multi-user network that consists of one BS and N terminal users.[4] Each user communicates with BS simultaneously over the same spectrum. Assuming a rich-scattering environment, each user's location is associated with a unique (effective) channel response $\tilde{h}_i(t)$, $i = 1, 2, \ldots, N$.

The channel probing occurs when a terminal user joins the network, and periodically afterwards.[5] The channel probing process is performed for one user at a time. For the ith user's channel probing, the terminal user first sends a pulse pilot signal $p(t)$ to the BS, so that the TR mirror at the BS can record and time reverse (and conjugate, if complex-valued) the received waveform $\tilde{h}_i(t)$, and use the TR waveform $\tilde{g}_i(t)$ as the basic signature waveform, given by[6]

$$\tilde{g}_i(t) = \frac{\tilde{h}_i^*(-t)}{\sqrt{\int_0^{T+T_P} |\tilde{h}_i(\tau)|^2 d\tau}}. \tag{11}$$

B. Data Transmission Phase—Downlink

After the channel recording phase, the system starts its data transmission phase. We first introduce the downlink scheme in this part. In the downlink scheme, at the BS, each of $\{X_1[k], X_2[k], \ldots, X_N[k]\}$ represents a sequence of information symbols that are independent complex random variables with zero mean. As shown in Fig. 8, we allow different users to adopt different rate backoff factors to accommodate the heterogeneous QoS requirement of the applications of IoT.

To implement the rate backoff, the ith sequence is first up-sampled by a factor of D_i at the BS, and the ith up-sampled sequence can be expressed as

$$X_i^{[D_i]}[k] = \begin{cases} X_i[k/D_i], & \text{if } k \bmod D_i = 0 \\ 0, & \text{if } k \bmod D_i \neq 0. \end{cases} \tag{12}$$

Then the up-sampled sequences are used to modulate the signature waveforms $\{\tilde{g}_1, \tilde{g}_2, \ldots, \tilde{g}_N\}$, by calculating the convolution of the ith up-sampled sequence $\{X_i^{[D_i]}[k]\}$ and the TR waveform $g_i(t)$ as shown in Fig. 8.

After that, all the signals are combined together, and the combined signal $S(t)$ to be transmitted is given by

$$\begin{aligned} S(t) &= \sum_{k \in \mathbb{Z}^+} \sum_{j=1}^{N} \beta_j X_j^{[D_j]}[k] \tilde{g}_j(t - kT_P) \\ &= \sum_{k \in \mathbb{Z}^+} \sum_{j=1}^{N} \beta_j X_j[k] \tilde{g}_j(t - kD_jT_P). \end{aligned} \tag{13}$$

[4] In this paper, users and devices are interchangeable.

[5] In general, the probing period depends on how fast the channel may vary.

[6] As we mentioned in Section II, we use the effective channel response for finite-bandwidth system.

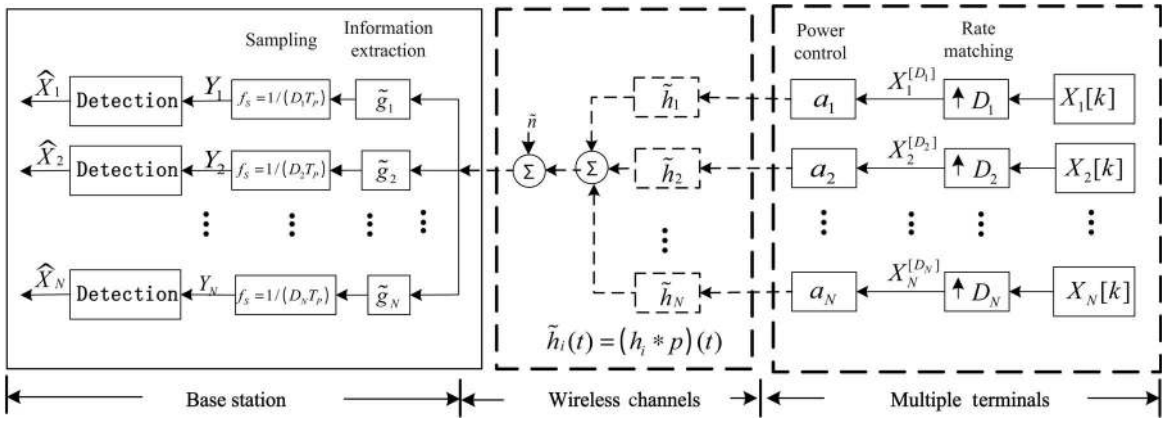

Fig. 9. Basic diagram of the TRDMA uplink.

In essence, by convolving the information symbol sequences with TR waveforms, the TR structure provides a mechanism of embedding the unique location-specific signature associated with each communication link into the transmitted signal for the intended user.

The signal received at user i is represented as follows:

$$\begin{aligned} Y_i(t) &= (S * \tilde{h}_i)(t) + \tilde{n}_i(t) \\ &= \sum_{k\in\mathbb{Z}^+} \sum_{j=1}^{N} \beta_j X_j[k](\tilde{h}_i * \tilde{g}_j)(t - kD_jT_P) + \tilde{n}_i(t) \end{aligned} \tag{14}$$

which is the convolution of the transmitted signal $S(t)$ and the channel response $\tilde{h}_i(t)$, plus an AWGN sequence $\tilde{n}_i(t)$ with zero mean and variance σ_N^2.

Thanks to the temporal focusing effect, the ith receiver (user i) simply samples the received signal every D_iT_P seconds at $t = kD_iT_P$, ending up with $Y_i[k]$ given as follows:

$$\begin{aligned} Y_i[k] &= \beta_i X_i[k](\tilde{h}_i * \tilde{g}_i)(0) && \text{Signal} \\ &+ \beta_i \sum_{\substack{l=-\left\lfloor \frac{T+T_P}{D_iT_P} \right\rfloor \\ l\neq 0}}^{\left\lfloor \frac{T+T_P}{D_iT_P} \right\rfloor} X_i[k+l](\tilde{h}_i * \tilde{g}_i)(lD_iT_P) && \text{ISI} \\ &+ \sum_{\substack{j=1 \\ j\neq i}}^{N} \beta_j \sum_{l=-\left\lfloor \frac{T+T_P}{D_jT_P} \right\rfloor}^{\left\lfloor \frac{T+T_P}{D_jT_P} \right\rfloor} X_j[k+l](\tilde{h}_i * \tilde{g}_j)(lD_jT_P) && \text{IUI} \\ &+ n_i[k] \end{aligned} \tag{15}$$

where $n_i[k] = \tilde{n}_i(kD_iT_P)$, and

$$(\tilde{h}_i * \tilde{g}_j)(lD_jT_P) = \begin{cases} \dfrac{\int_{lD_jT_P}^{T+T_P} \tilde{h}_i(\tau)\tilde{h}_j(\tau - lD_jT_P)d\tau}{\sqrt{\int_0^{T+T_P} |\tilde{h}_j(\tau)|^2 d\tau}}, & \text{if } 0 \leqslant l \leqslant \left\lfloor \frac{T+T_P}{D_jT_P} \right\rfloor \\ \dfrac{\int_0^{T+T_P+lD_jT_P} \tilde{h}_i(\tau)\tilde{h}_j(\tau - lD_jT_P)d\tau}{\sqrt{\int_0^{T+T_P} |\tilde{h}_j(\tau)|^2 d\tau}}, & \text{if } \left\lfloor \frac{T+T_P}{D_jT_P} \right\rfloor \leqslant l < 0. \end{cases} \tag{16}$$

Thanks to the spatial focusing effect, in (16), when $i \neq j$, the power of $(\tilde{h}_i * \tilde{g}_j)(lD_jT_P)$ is typically very small compared to the power of the $(\tilde{h}_i * \tilde{g}_i)(0)$, which suppresses the inter-user-interference (IUI) for the TRDMA downlink.

Consequently, based on (15), the resulting SINR for user i in the TRDMA downlink is given by

$$\mathrm{SINR}_{\mathrm{DL}}^{(i)} = \frac{P_{\mathrm{sig}}^{\mathrm{DL}}(i)}{P_{\mathrm{ISI}}^{\mathrm{DL}}(i) + P_{\mathrm{IUI}}^{\mathrm{DL}}(i) + \sigma_N^2} \tag{17}$$

where

$$P_{\mathrm{Sig}}^{\mathrm{DL}}(i) = \beta_i^2 \int_0^{T+T_P} |\tilde{h}_i(\tau)|^2 d\tau \tag{18}$$

$$P_{\mathrm{ISI}}^{\mathrm{DL}}(i) = \beta_i^2 \sum_{\substack{l=-\left\lfloor \frac{T+T_P}{D_iT_P} \right\rfloor \\ l\neq 0}}^{\left\lfloor \frac{T+T_P}{D_iT_P} \right\rfloor} |(\tilde{h}_i * \tilde{g}_i)(lD_iT_P)|^2 \tag{19}$$

and

$$P_{\mathrm{IUI}}^{\mathrm{DL}}(i) = \sum_{\substack{j=1 \\ j\neq i}}^{N} \beta_j^2 \sum_{l=-\left\lfloor \frac{T+T_P}{D_jT_P} \right\rfloor}^{\left\lfloor \frac{T+T_P}{D_jT_P} \right\rfloor} |(\tilde{h}_i * \tilde{g}_j)(lD_jT_P)|^2. \tag{20}$$

C. Data Transmission Phase—Uplink

In this part, we describe the TRDMA uplink scheme, which facilitated, together with the downlink scheme, the asymmetric TRDMA architecture for IoT. Given the asymmetric complexity distribution between BS and terminal users in the downlink, the design philosophy of such a uplink is to keep the complexity of terminal users at minimal level.

In the TRDMA uplink, N users simultaneously transmit independent messages $\{X_1[k], X_2[k], \ldots, X_N[k]\}$ to the BS through the multi-path channels. Similar to the downlink scheme, the rate backoff factor D is introduced to match the symbol rate with the system's chip rate. For any user U_i, $i \in \{1, 2, \ldots, N\}$, the rate matching process is performed by up-sampling the symbol sequence $\{X_i[k]\}$ by a factor D_i, as shown in Fig. 9.

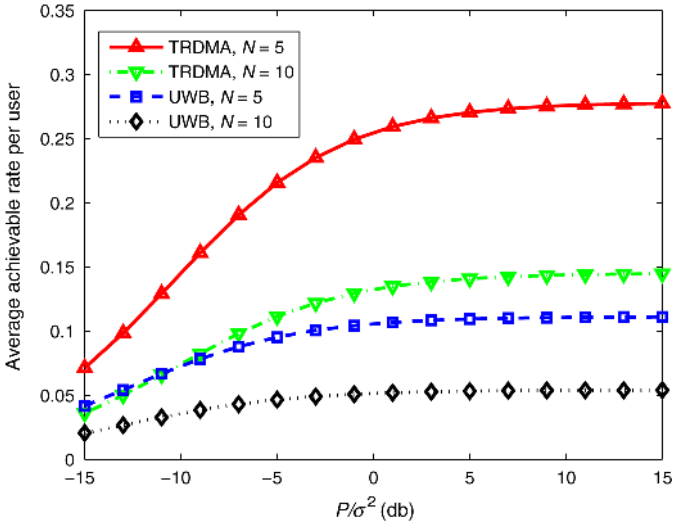

Fig. 10. Performance comparison between TRDMA and UWB in terms of average achievable data rate per user.

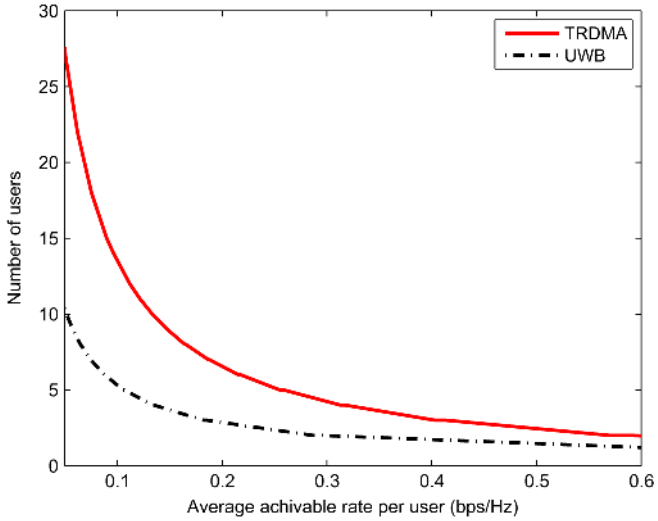

Fig. 11. Performance comparison between TRDMA and UWB in terms of number of supported users.

The up-sampled sequence of modulated symbols for user can be expressed as

$$X_i^{[D_i]}[k] = \begin{cases} X_i[k/D_i], & \text{if } k \bmod D_i = 0 \\ 0, & \text{if } k \bmod D_i \neq 0. \end{cases} \tag{21}$$

The scaling factors a_i, for $i \in \{1, 2, \ldots, N\}$ in Fig. 9, are used to implement the transmit power control, whose values are assumed to be instructed by the BS through the feedback/control channel. After multiplying with scaling factor, the sequence of $a_i X_i^{[D_i]}[k]$ for all $i \in \{1, 2, \ldots, N\}$ is transmitted through the corresponding multi-path channel $\tilde{h}_i(t)$.

When the sequence $\{a_i X_i^{[D_i]}[k]\}$ propagates through its wireless channel $\tilde{h}_i(t)$, the convolution between $\{a_i X_i^{[D_i]}[k]\}$ and the effective channel response $\{h_i[k]\}$ is automatically taken as the channel output for user i. Then, all of the channel outputs for the N users are mixed together in the air plus the AWGN $\tilde{n}[k]$ at the BS with zero mean and variance σ_N^2, as illustrated in Fig. 9. Consequently, the mixed signal received at the BS can be written as

$$S(t) = \sum_{k \in \mathbb{Z}^+} \sum_{i=1}^{N} a_i X_i[k] \tilde{h}_i(t - kD_i T_P) + \tilde{n}(t). \tag{22}$$

Upon receiving the mixed signal as shown in (22), the BS passes this mixed signal through a bank of N filters, each of which performs the convolution between its input signal $S(t)$ and the user's signature waveform $\tilde{g}_i(t)$ that has been calculated for the downlink. Such a convolution using the signature waveform extracts the useful signal component and suppresses the signals of other users. As the output of the ith filter, i.e., the convolution of $S(t)$ and the signature of user i, $\tilde{g}_i(t)$ can be represented as

$$Y_i(t) = \sum_{k \in \mathbb{Z}^+} \sum_{j=1}^{N} a_j X_j[k] (\tilde{g}_i * \tilde{h}_j)(t - kD_j T_P) + (\tilde{g}_i * \tilde{n})(t) \tag{23}$$

in which the highest gain for user i's symbol $X_i[k]$ is achieved at the temporal focusing time $t = kD_i T_P$.

Sampling $Y_i(t)$ every $D_i T_P$ seconds at $t = kD_i T_P$, we have

$$\begin{aligned} Y_i[k] = {} & a_i X_i[k](\tilde{g}_i * \tilde{h}_i)(0) && \text{Signal} \\ & + a_i \sum_{\substack{l=-\left\lfloor \frac{T+T_P}{D_i T_P} \right\rfloor \\ l \neq 0}}^{\left\lfloor \frac{T+T_P}{D_i T_P} \right\rfloor} X_i[k+l](\tilde{h}_i * \tilde{g}_i)(lD_i T_P) && \text{ISI} \\ & + \sum_{\substack{j=1 \\ j \neq i}}^{N} a_j \sum_{l=-\left\lfloor \frac{T+T_P}{D_j T_P} \right\rfloor}^{\left\lfloor \frac{T+T_P}{D_j T_P} \right\rfloor} X_j[k+l](\tilde{h}_j * \tilde{g}_i)(lD_j T_P) && \text{IUI} \\ & + n_i[k] \end{aligned} \tag{24}$$

where $n_i[k] = (\tilde{g}_i * \tilde{n})(kD_i T_P)$ is a sample of the colored noise after the $\tilde{g}_i(t)$ filtering, which is still a Gaussian random variable with zero mean and the same variance σ_N^2, since $\tilde{g}_i$ is a normalized waveform as shown in (11).

Examining (15) and (24), the same mathematical structure can be found by switching the roles of the signature waveforms $\tilde{g}_i$'s and the channel responses $\tilde{h}_i$'s in the convolution (and ignoring the scaling factor a_i and noise term.) Therefore, mathematically,[7] a virtual spatial focusing effect as observed in the downlink can be seen in the user's signature domain of the proposed uplink scheme. Such a virtual spatial focusing effect enables the BS to use the user's signature waveform to extract the useful component out of the combined received signals, allowing multiple users to access the BS simultaneously.

[7]Unlike the *physical* spatial focusing effect observed in the downlink in which the useful signal power is concentrated at different physical locations, in the uplink, the signal power concentration in the users' signature waveform space is achieved mathematically at the BS.

Consequently, based on (24), the resulting SINR for user i in the TRDMA uplink is given by

$$\mathrm{SINR}_{\mathrm{UL}}^{(i)} = \frac{P_{\mathrm{sig}}^{\mathrm{UL}}(i)}{P_{\mathrm{ISI}}^{\mathrm{UL}}(i) + P_{\mathrm{IUI}}^{\mathrm{UL}}(i) + \sigma_N^2} \tag{25}$$

where

$$P_{\mathrm{Sig}}^{\mathrm{UL}}(i) = a_i^2 \int_0^{T+T_P} |\tilde{h}_i(\tau)|^2 d\tau \tag{26}$$

$$P_{\mathrm{ISI}}^{\mathrm{UL}}(i) = a_i^2 \sum_{\substack{l=-\left\lfloor \frac{T+T_P}{D_i T_P} \right\rfloor \\ l\neq 0}}^{\left\lfloor \frac{T+T_P}{D_i T_P} \right\rfloor} |(\tilde{h}_i * \tilde{g}_i)(lD_i T_P)|^2 \tag{27}$$

and

$$P_{\mathrm{IUI}}^{\mathrm{UL}}(i) = \sum_{\substack{j=1 \\ j\neq i}}^{N} a_j^2 \sum_{l=-\left\lfloor \frac{T+T_P}{D_j T_P} \right\rfloor}^{\left\lfloor \frac{T+T_P}{D_j T_P} \right\rfloor} |(\tilde{h}_j * \tilde{g}_i)(lD_j T_P)|^2. \tag{28}$$

D. Performance of TRDMA

In this section, we compare the performance of the proposed TRDMA system with that of the UWB impulse radio system in terms of different metrics, where we assume that the UWB impulse radio system uses the ideal Rake receiver that collects all the taps of channel information. We first compare the average achievable data rate of each user when the power consumption is the same for two systems. As shown in Fig. 10, the TRDMA system is able to provide higher achievable data rate for each user than the UWB impulse radio system.

We then evaluate the number of users where each system can support. Since TRDMA mitigates the interference among users, it is expected to be able to support more users. In Fig. 11, we show the number of supported users versus the average achievable rate of each user. We can see that, as we have anticipated, the TRDMA system is able to support more users than the UWB impulse radio system. For example, if the required data rate of each user is 0.1 bps/Hz, which is equivalent to 10 Mbps if the bandwidth is 100 MHz, then the TRDMA system can support about 20 users while the UWB impulse radio system can support only five users.

On the other hand, if the achievable data rate of each user is fixed, the TRDMA system has less impact on the neighboring users, i.e., causing less interference to users outside the system. As shown in Fig. 12, when we fix the achievable rate of each user as 0.1 bps/Hz, the performance degradation due to the TRDMA system is much less than that of UWB impulse radio system. Therefore, the TRDMA system has the potential to admit more users and thus is a much better solution to the IoT.

Finally, we show the achievable rate region of two-user case in Fig. 13, where we further compare the proposed TRDMA system with ideal rake-receiver schemes with orthogonal bases and superposition codes [25]. We can see that the proposed TRDMA scheme outperforms all the rake-receiver-based schemes, and the

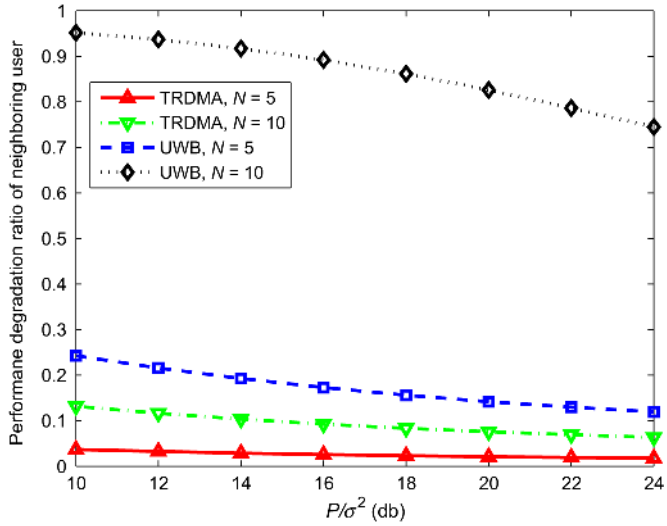

Fig. 12. Impact to other users outside the system.

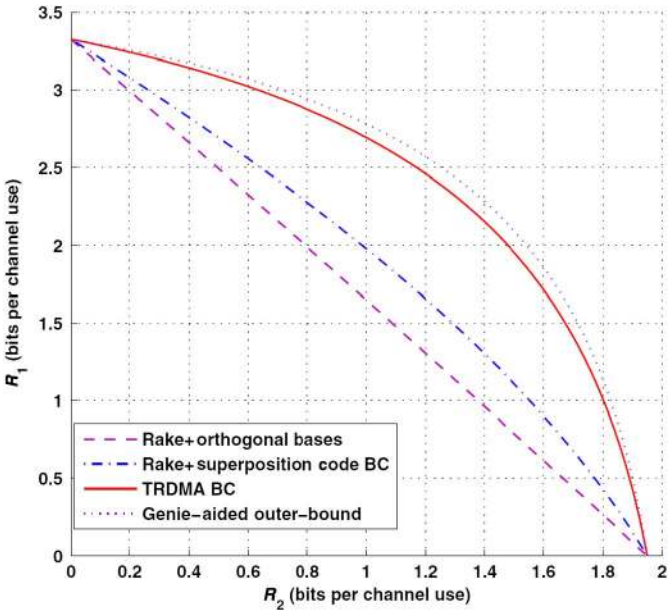

Fig. 13. Achievable capacity region for two-user case [25].

frontier achieved by TRDMA scheme is close to the Genie-aided outer-bound where all the interference is assumed to be known and thus can be completely removed. These results demonstrate TRDMA's unique advantage of spatial focusing brought by the pre-processing of embedding location-specific signatures before sending signals into the air. The high-resolution spatial focusing, as the key mechanism of the TRDMA, alleviates interference among users and provides a promising multi-user wireless communication solution for IoT.

E. Scalability

In the previous sections, we have shown that a single TRDMA BS has the potential to serve a lot of users while maintaining little interference to other wireless users. However, in IoT applications, the density of users may be so high that one single BS is insufficient to support all of them. One possible solution is to

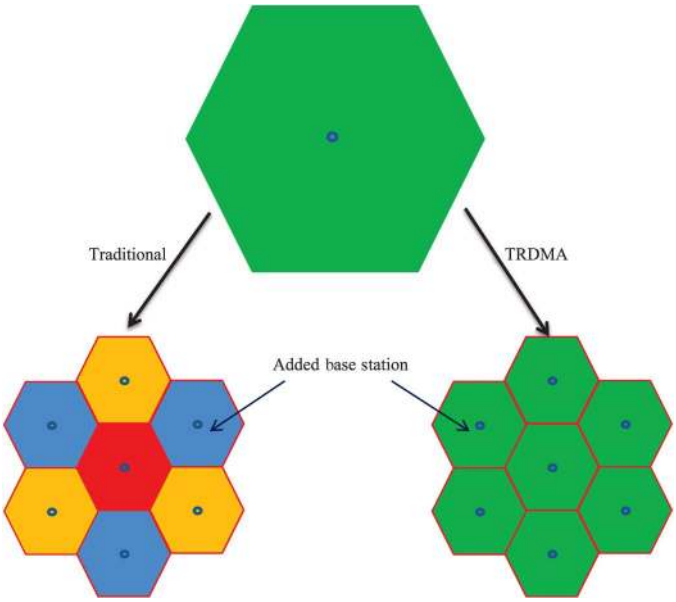

Fig. 14. Illustration of spectrum re-use in TRDMA system.

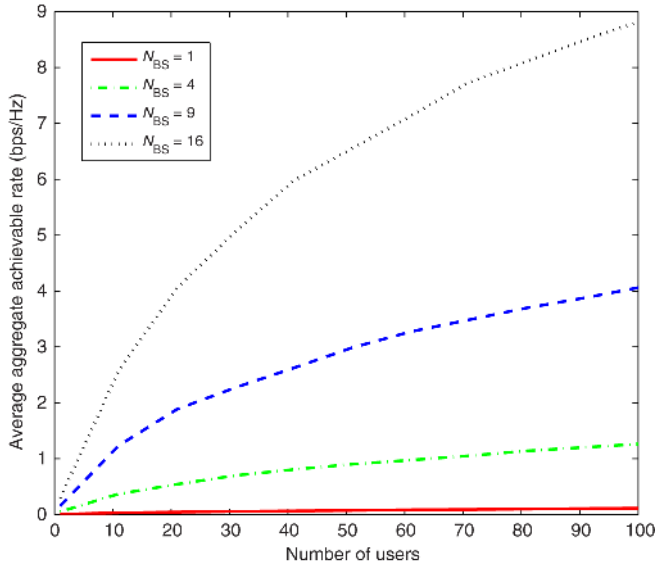

Fig. 15. Scalability performance of the TRDMA system.

add more BSs, and we will show that the TRDMA system is highly scalable and extra BSs can be easily installed whenever necessary.

Different from other wireless communication systems where extra mechanism is needed to prevent or alleviate the interference introduced by adding more BSs, the TRDMA system does not need extra effort on suppressing the interference introduced by more BSs due to the spatial focusing effect. As an example shown in Fig. 14, if six more BSs are added surrounding the original one, all of them could use the full spectrum as the original one in the TRDMA system, while in other systems the spectrum needs to be re-allocated so that no adjacent BSs share the same band. This ease of scalability also increases the spectrum efficiency by fully reusing spectrum among BSs.

Fig. 15 shows the aggregate achievable data rate versus the number of users at different number of BSs. We can see that given a specific number of BSs, the aggregate achievable rate increases as the number of users increases, but saturates when the number of users is large. Nevertheless, such saturation can be resolved by increasing the number of BSs, which means that adding more BSs can bring significant gain. This is partially because although different BSs share the same spectrum, they are nearly orthogonal with each other. Such orthogonality is not in the traditional fashion such as time, code or frequency divisions that are achieved by extra effort, but in a natural spatial division that is only utilized by TRDMA system.

F. Physical-Layer Security

Based on the unique location-specific multi-path profile, the TRDMA system can be exploited to enhance system security. In a rich scattering wireless environment, multiple paths are formed by numerous surrounding reflectors. For terminal devices at different locations, the received waveforms undergo different reflecting paths and delays, and hence the multi-path profile can be viewed as a unique location-specific signature. As this information is only available to the BS and the intended terminal device, it is very difficult for other unauthorized users to infer or forge such a signature. It has been shown in [64] that even when the eavesdroppers are close to the target terminal device, the received signal strength is much lower at the eavesdroppers than at the target terminal device in an indoor application, because the received signals are added incoherently at the eavesdroppers.

Our TRDMA system is somehow like the direct sequence spread spectrum (DSSS)-based secret communications. In DSSS communications, the energy of an original data stream is spread to a much wide spectrum band by using a pseudo-random sequence, and the signal is hidden below the noise floor. It is only those who know the pseudo-random sequence that could recover the original sequence from the noise-like signals. However, if the pseudo-random sequence has been leaked to a malicious user, that user is also capable of decoding the secret message. Nevertheless, for our proposed TRDMA system, this would no longer be a problem, because the underlying spreading sequence is not a fixed choice but instead a location-specific signature. For the intended terminal device, the multi-path channel automatically serves as a decipher that recovers the original data sent by the BS; and for all other ineligible users at different locations, the signal that propagates to them would be noise-like and probably is hidden below the noise floor. Therefore, malicious users are unable to recover the secret message, because the security is inherent in the physical layer.

G. Discussions and Remarks

From the analysis and discussions in the previous sections, we can see that the asymmetric TRDMA system is an ideal wireless solution to the IoT since it can handle the challenges of IoT including providing better battery life, supporting multiple active things, dealing with low-cost terminal devices, accommodating heterogeneous terminal devices, being highly scalable, and providing extra physical-layer security as summarized below.

1) In both downlink and uplink, the BS consumes most of the complexities, while keeping the complexity of terminal users at a minimal level. This is a very desirable feature for

the solution to IoT since it can provide much better battery life and reduce the cost of the terminal devices and thus the entire system as a whole.

2) Both downlink and uplink can support simultaneous transmissions of multiple users since the TRDMA system in essence forms a virtual massive MISO technology that leverages the large number of multi-paths in the rich-scattering environment. The downlink has a physical spatial focusing effect; whereas the uplink has a virtual spatial focusing effect due to the mathematical duality between the TRDMA uplink and downlink.
3) Different users can adopt different rate backoff factors to achieve heterogeneous QoS requirements, i.e., the TRDMA system can accommodate heterogeneous terminal devices for IoT.
4) More BSs can be easily added in the TRDMA system without extra mechanism for preventing or alleviating the interference introduced, i.e., the TRDMA system is highly scalable.
5) Based on the unique location-specific multi-path profile, the TRDMA system can provide extra system security in the physical layer.

IV. Other Challenging Issues and Future Directions

A. Advanced Waveform Design

In our discussion of TRDMA in the previous section, the TR CIR serves as the transmit signature waveform to modulate symbols. The received signal is the transmitted waveform convolving with the multi-path channel with additive noise. Such a time-reversed waveform is essentially the matched filter [65], which guarantees the optimal BER performance by virtue of its maximum signal-to-noise ratio (SNR). However, in high data rate scenario such as video streaming, when the symbol duration is smaller than the channel delay spread, the transmit waveforms are overlapped and thus interfere with each other. When the symbol rate is very high, such ISI can be notably severe and causes crucial performance degradation, i.e., the BER performance can be very poor with a basic time-reversed waveform. Further, in multi-user downlink scenario, the TR BS uses each user's particular CIR as its specific waveform to modulate the symbols intended for that user. Despite the inherent randomness of the CIRs, as long as they are not orthogonal to each other, which is almost always the case, these waveforms will inevitably interfere with each other when transmitted concurrently. Hence, the performance of TRDMA can be impaired and even limited by the IUI.

Based on given design criteria such as system performance, QoS constraints, or fairness among users, the waveform design can be formulated as an optimization problem with the transmitted waveforms as the optimization valuables. The basic idea of waveform design is to carefully adjust the amplitude and phase of each tap of the waveform based on the channel information, such that after convolving with the channel, the received signal at the receiver retains most of the intended signal strengths and rejects or suppresses the interference as much as possible.

To rewrite (15) in a vector from, we define the following notations. The multipath channel between the base-station and the jth user is denoted by a vector $\boldsymbol{h}_j$, a column vector of $\boldsymbol{L}$ elements where $\boldsymbol{L} = \left\lfloor \frac{T+T_P}{T_P} \right\rfloor$ and $[\boldsymbol{h}_j]_k = \tilde{h}_j(t)|_{t=kT_P}$. Let X_j denote an information symbol for user j, and $\boldsymbol{g}_j$ be the transmit waveform for user j, where $[\boldsymbol{g}_j]_k = \tilde{g}_j(t)|_{t=kT_P}$ in (15). The length of $\boldsymbol{g}_k$ is also $\boldsymbol{L}$. The received signal vector $\boldsymbol{y}_i$ at user i, where $[\boldsymbol{y}_i]_k = Y_i[k]$ in (15), is given by

$$\boldsymbol{y}_i = \boldsymbol{H}_i \sum_{j=1}^{N} \boldsymbol{g}_j X_j + \boldsymbol{n}_i \tag{29}$$

where $\boldsymbol{H}_i$ is the Toeplitz matrix of size $(2L-1) \times L$ with the first column being $[\boldsymbol{h}_i^T \ \boldsymbol{0}_{1\times(L-1)}]^T$, and $\boldsymbol{n}_i$ denotes the AWGN with $[\boldsymbol{n}_i]_k = n_i[k]$. User i estimates the symbol X_i by the sample $[y_k]_L$. Note that (29) represents the received signal when the rate backoff factor $D > L$. When $D < L$, the received waveforms of different symbols overlap with each other and give rise to the ISI. To characterize the effect of ISI, the decimated channel matrix of size $(2L_D - 1) \times L$, where $L_D = \left\lfloor \frac{L-1}{D} \right\rfloor + 1$, is defined as

$$\tilde{\boldsymbol{H}}_i = \sum_{l=-L_D+1}^{L_D-1} \boldsymbol{e}_{L_D+l} \boldsymbol{e}_{L+lD}^T \boldsymbol{H}_i \tag{30}$$

where e_l is the lth column of a $(2L-1) \times (2L-1)$ identity matrix. In other words, $\tilde{\boldsymbol{H}}_i$ is obtained by decimating the rows of $\boldsymbol{H}_i$ by D, i.e., centering at the Lth row, every Dth row of $\boldsymbol{H}_i$ is kept in $\tilde{\boldsymbol{H}}_i$ while the other rows are discarded. The center row index of $\tilde{\boldsymbol{H}}_i$ is L_D. Then the sample for symbol estimation can be written as

$$\begin{aligned}[\boldsymbol{y}_i]_L = {} & \boldsymbol{h}_{iL}^H \boldsymbol{g}_i X_i[L_D] + \boldsymbol{h}_{iL}^H \sum_{j\neq i} \boldsymbol{g}_j X_j[L_D] \\ & + \sum_{l=1, l\neq L_D}^{2L_D-1} \boldsymbol{h}_{il}^H \sum_{j=1}^{N} \boldsymbol{g}_j X_j[l] + n_i[L]\end{aligned} \tag{31}$$

where $\boldsymbol{h}_{il}^H = \mathbf{e}_l^T \tilde{\boldsymbol{H}}_i$ denotes the lth row of $\tilde{\boldsymbol{H}}_i$, and $X_j[l]$ denotes user j's lth symbol. It can be seen from (31) that the symbol $X_i[L_D]$, the L_Dth symbol of user i, is interfered by the previous $L_D - 1$ symbols and the later $L_D - 1$ symbols as well as other users' $K(2L_D - 1)$ symbols, and also corrupted by the noise. The design of waveforms $\{\boldsymbol{g}_i\}$ has critical influence to the symbol estimation and thus the system performance.

It can be observed that the mathematical structure of waveform design is similar to the beamforming problem, which is also known as the multi-antenna precoder design [66]–[70]. Therefore, beamforming approaches, such as singular value decomposition (SVD), zero forcing (ZF), and minimal mean square error (MMSE), can be analogously employed in waveform design. In the literature, there have been many studies investigating the problems of designing advanced waveforms to suppress the interference [27], [46], [71]–[76]. If the basic TR waveforms are adopted, i.e., $\boldsymbol{g}_i = \boldsymbol{h}_{iL}$, then the intended signal power for each user is maximized but without considering the interference caused by other symbols. As such, the performance is limited by the interference when the transmit power is high. Another possible waveform design is ZF [77], which minimizes all the interference signal power but without taking into account

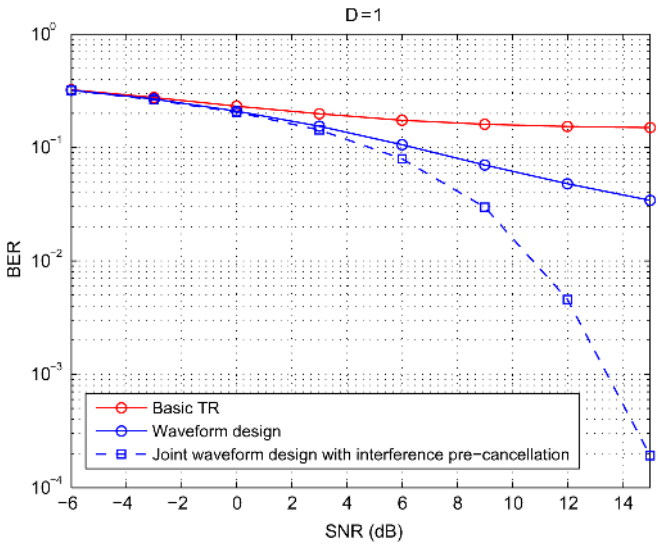

Fig. 16. BER performance comparison using basic TR waveform, waveform design, and joint waveform design and interference pre-cancelation.

the intended signal power. Thus, the resulting SNR can be very low and causes severe performance degradation especially when the transmit power is relatively low. In [27], it has been shown that well-designed waveforms can strike a balance between enhancing the intended signal power and suppressing the interference power.

Besides the channel information, another important side information the transmitter can exploit in waveform design, is the transmitted symbol information. The waveform of one symbol, when arriving at the receiver, induces ISI to the previous symbols as well as the following symbols. Given what has been transmitted, the causal part of ISI can be canceled in advance in designing the waveform of the current symbol. Such a design pholosophy is analogous to the transmitter-based interference pre-subtraction [78]–[80] in the nonlinear precoding literature. A notable distinction for TR systems is that only the causal part of ISI can be canceled while the anti-causal part of ISI cannot be canceled and needs to be suppressed by the waveform design based on channel information [49].

Fig. 16 shows the BER performance for a single user TR system when $D = 1$ using different waveforms, including basic TR waveform, the waveform design in [27], and the joint waveform design and interference pre-cancelation in [49]. It can be seen that when $D = 1$, the ISI is so severe that the BER curve of the basic TR waveform starts to saturate at even middle SNR, which is unacceptable. The waveform design in [27] is able to suppress the interference and make the BER keep decreasing when SNR increases. The joint waveform design and interference pre-cancelation in [49] can further improve the performance significantly since it makes use of more information, i.e., the transmitted symbols, to cancel the ISI in advance. It is evident that the dramatic performance improvement brought from the waveform design demonstrates its inevitable necessity in TR systems.

Fig. 17 shows the performance comparison in terms of achievable rate of the TRDMA system with 500-MHz bandwidth with two OFDM systems: one is LTE system with 20-MHz bandwidth and the other is LTE-A system with 100-MHz bandwidth. We can see that for one user case, even with basic TR waveform, the TRDMA scheme can achieve much better performance than LTE in all SNR region and better performance than LTE-A in most SNR region. With optimal waveform, the performance of TRDMA can be further improved. When there are 10 users, due to the selectivity among different users, the achievable rate of LTE and LTE-A can be enhanced, due to which LTE-A can achieve comparable and even slightly better performance than TRDMA with basic TR waveform. Nevertheless, with optimal waveform, TRDMA can still outperform LTE and LTE-A in most SNR region, which demonstrates that TRDMA can achieve higher throughput than OFDM systems when the bandwidth is wide enough, e.g., five times as in the simulations.

B. Medium Access Control (MAC) Layer Issue

The MAC layer provides addressing and channel access control mechanisms that make it possible for several terminals or network nodes to communicate within a multiple access network that incorporates a shared medium [81]. In the MAC layer design, coordination is the most basic and important function, which manages multiple users to access the network with the objective of both efficiency and fairness. Most of the existing prevailing systems, such as IEEE 802.11 WiFi and IEEE 802.15.4 ZigBee, are based on the contention scheme. For example, in WiFi systems, distributed coordination function (DCF) is adopted with Carrier Sensing Multiple Access (CSMA) and Collision Avoidance (CA) [82]. When a WiFi user has packet to transmit, it first senses the channel, i.e., "Listen-Before-Talk." After detecting the channel as idle, the WiFi user has to keep sensing the channel for an additional random time [83], i.e., random backoff and only when the channel remains idle for this additional random time period, the station is allowed to initiate its transmission. If there is a collision, the user needs to backoff and repeat this procedure again. Under such a scheduling, there is only one WiFi user talking with the AP at one time. However, when the number of users is large, no one can access the network due to the contention failure and extremely long backoff. We have all seen and experienced such a phenomenon in highly dense-population area including airport and conference hall. A typical example is that Steve Jobs failed to demo the WiFi function of the new released iPhone due to the overwhelming connections in the conference room [84]. Therefore, such a contention-based coordination function of the MAC layer is a bottleneck for accommodating large number of users, which generally exists in IoT.

The most prominent characteristic of the TR system is that it does not require such coordination function, where users are naturally separated by their locations. There are two phases in the TR systems: channel probing phase and data transmission phase. In the channel probing phase, all the users can transmit their unique pilots (e.g., pseudo-noise sequences) to the BS for channel estimation. In the data transmission phase, BS can communicate with all the users simultaneously through location-specific signatures. Therefore, there is no need for the BS in TR systems to perform coordination function, which simplify the MAC layer design to a large extent. In addition to coordination, some additional functionalities required by the MAC are also needed in TR systems, including accepting MAC Service Data

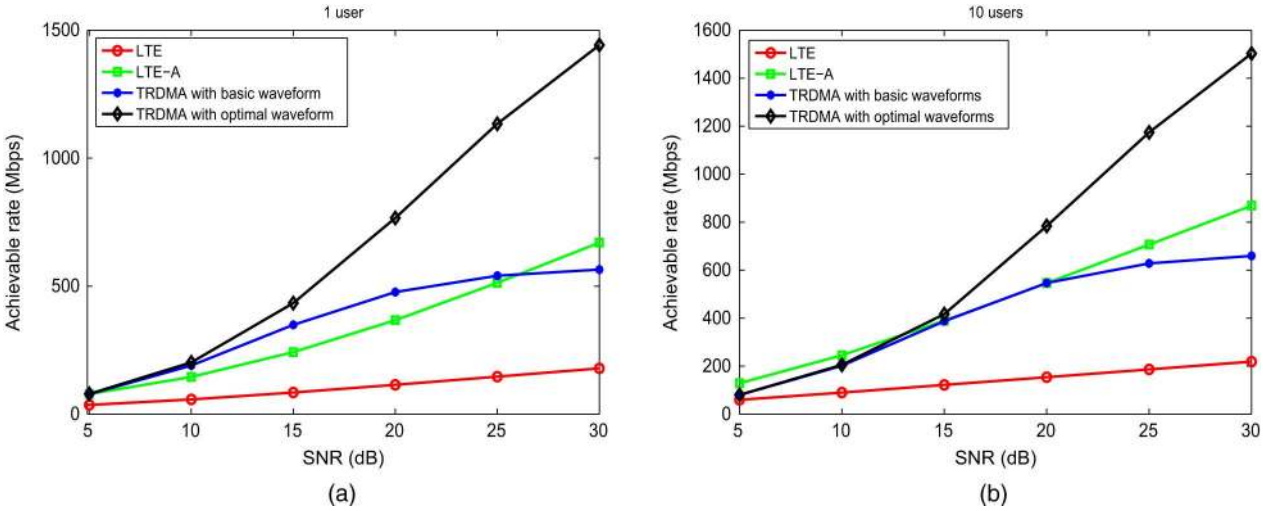

Fig. 17. Achievable rate comparison: (a) 1 user case and (b) 10 users case.

Units (MSDUs) from higher layers and adding headers and trailers to create MAC protocol data unit (MPDU) for physical layer, fragmenting one frame into several frames to increase the delivery probability, and encrypting MAC layer packet to ensure security and privacy [83]. Nevertheless, we would like to emphasize again that the location-specific signature in TR systems can provide additional physical-layer security.

C. Low-Cost High-Speed ADC and DAC

The inherent nature of TR communications is to fully harvest energy from the surrounding environment by exploiting the multi-path propagation to re-collect all the signal energy that could be collected. To have superior advantage, the TR communications need to operate in a rich multi-path environment, which generally require wide bandwidth. As a consequence, the sampling rate is typically high. Moreover, to avoid missing the peak during the sampling and simplify the synchronization process, a two to four times oversampling is generally required, which make the sampling even more challenging. Therefore, one key implementation issue in TR communications is the high sampling rate of the ADC. Fortunately, due to the advance of semiconductor technologies and the continuous driven from the emerging wideband communication applications, the performance of ADC has been improved a lot during the past decade in terms of both sampling rate and resolution. For example, there are 17 different commercial off-the-shelf ADCs from Texas Instrument with sampling rate at least 1 GHz and resolution at least 8 bits [85]. However, the price of such ADCs is typically high, e.g., an ADC with two-channel 2-GHz sampling rate and 8 bits resolution costs US$329, which may barrier the application of TR technique on IoT. In such a case, there is a need to find cheaper solutions to high sampling rate ADCs.

There are two possible ways to reduce the cost of high sampling rate ADCs. The first way is to implement the ADC on chip. In such a case, the cost of ADC comes from the silicon cost, which depends on silicon wafer cost and the size of the ADC on silicon. In general, with silicon implementation, the cost of ADC can be reduced from several hundred dollars to several cents without considering the capital cost. Nevertheless, since the capital cost is typically very high, such kind of implementation is only suitable for large volume productions. The other way to reduce the cost is using a set of low sampling rate cheap ADCs to achieve the high sampling rate. As the price of commercial ADCs grows exponentially with the increase in sampling rate, by replacing the high sampling rate ADCs with a set of low sampling rate ADCs, the cost can be reduced dramatically. One straightforward way is to use time interleaving [86], [87]. In such an approach, the input signal is passed through a series of parallel interleaved low sampling rate ADCs where the interleaving is achieved through the time shifts. After the sampling, the samples are passed through the de-interleaver to generate the high sampling rate signal. However, the front end of a commercial ADC has an inherent analog bandwidth limitation [88], [89], due to which the time interleaving approach is not practical. The second approach is to use parallel bandpass sampling approach [90], [91] where the input signal is passed through a series of filter bank before the ADCs and the reconstruction method depends on the corresponding filters in the filter bank. This kind of approach can resolve the analog bandwidth limitation but necessitates sophisticated digital algorithms for accurate frequency synchronization. Another approach is to use random demodulation [92], [93] where the input signal is passed through parallel channels. In each channel, the input signal is first multiplied by a periodic random waveform in the analog domain, then lowpass filtered, and finally sampled using low sampling rate ADC. The random demodulation approaches overcomes the disadvantages of the time interleaving approach and the parallel bandpass sampling approach, but is limited by the technology for generating the periodic random waveforms. Note that in all these approaches, the costly high sampling rate ADC is traded with the computation complexity for reconstruction in digital domain which is relatively cheap.

V. Conclusion

In this paper, we provide an overview to show that the TR technique is an ideal paradigm for IoT. Because of the inherent nature to fully harvest energy from the surrounding environment

by exploiting the multi-path propagation to recollect all the signal energy, the TR system has a potential of over an order of magnitude of reduction in power consumption and interference alleviation, which means that TR system can provide better battery life and support multiple concurrent active users. The unique asymmetric architecture proposed in this paper can significantly reduce the computational complexity and thus the cost of the terminal devices, the total number of which is typically very large for IoT. Moreover, through adjusting the waveform and rate backoff factor, various QoS options can be easily supported in TR systems. Finally, the unique location-specific signature in TR system can provide additional physical-layer security and thus can enhance the privacy and security of customers in IoT. All these advantages, including providing better battery life, supporting multiple active things, dealing with low-cost terminal devices, accommodating heterogeneous terminal devices, being highly scalable and providing extra physical-layer security, show that the TR technique is an ideal paradigm for IoT.

Recently, researchers start to envision the next major phase of mobile telecommunications standards beyond current 4G standards, known as 5G. According to [94], key concepts of 5G include new modulation techniques such as non-orthogonal multiple access schemes, massive distributed MIMO, advanced interference management, and efficient support of machine-type devices to enable the IoT with potentially higher numbers of connected devices. Based on the discussion in this paper, it turns out that TR can easily resolve these issues, which means that TR is potentially a promising 5G technology.

References

[1] G. Kortuem, F. Kawsar, D. Fitton, and V. Sundramoorthy, "Smart objects as building blocks for the internet of things," *IEEE Internet Comput.*, vol. 14, no. 1, pp. 44–51, Feb. 2010.

[2] C. Institutes, "Smart networked objects and internet of things," in *Proc. Inf. Commun. Technol. Micro Nano Technol. Alliance*, White Paper, Jan. 2011.

[3] L. Atzori, A. Iera, and G. Morabito, "The internet of things: A survey," *Comput. Netw.*, vol. 54, no. 15, pp. 2787–2805, Oct. 2010.

[4] D. Le-Phuoc, A. Polleres, M. Hauswirth, G. Tummarello, and C. Morbidoni, "Rapid prototyping of semantic mash-ups through semantic web pipes," in *Proc. 18th Int. Conf. World Wide Web*, 2009, pp. 581–590.

[5] A. Dohr, R. Modre-Opsrian, M. Drobics, D. Hayn, and G. Schreier, "The internet of things for ambient assisted living," in *Proc. Int. Conf. Inf. Technol.: New Gener.* (ITNG), 2010, pp. 804–809.

[6] European Commission, "Internet of things in 2020 road map for the future," *Working Group. RFID of the ETP EPOSS, Tech. Rep., May 2008.*

[7] K. Ashton, "That 'internet of things' thing in the real world, things matter more than ideas," *RFID J.,* Jun. 2009.

[8] D. L. Brock, "The electronic product code (epc) a naming scheme for physical objects," Auto-ID Center, White Paper, Jan. 2001.

[9] I. T. Union, "ITU internet reports 2005: The internet of things," in *Proc. Workshop Rep. Int. Telecommun. Union*, Nov. 2005.

[10] P. Guillemin and P. Friess, "Internet of things strategic research roadmap," *The Cluster of European Research Projects*, Tech. Rep., Sep. 2009.

[11] C. Gomez and J. Paradells, "Wireless home automation networks: A survey of architectures and technologies," *IEEE Commun. Mag.*, vol. 48, no. 6, pp. 92–101, Jun. 2010.

[12] J. Berman, "Z-wave chip aims to cut implementation cost," *EDN Netw.*, pp. 92–101, Apr. 2005.

[13] *IEEE Standard for Telecommunications and Information Exchange Between Systems—lan/man—Specific Requirements—Part 15: Wireless Medium Access Control (mac) and Physical Layer (phy) Specifications for Wireless Personal Area Networks (wpans)*, IEEE 802.15.1-2002 [Online]. Available: http://ieeexplore.ieee.org/xpl/mostRecentIssue.jsp?punumber=7932

[14] *Wireless lan Medium Access Control (mac) and Physical Layer (phy) Specification*, IEEE 802.11 [Online]. Available: http://standards.ieee.org/getieee802/download/802.11-2012.pdf

[15] L. Li, X. Hu, K. Chen, and K. He, "The applications of wifi-based wireless sensor network in internet of things and smart grid," in *Proc. IEEE Conf. Ind. Electron. Appl.* (ICIEA), 2011, pp. 789–793.

[16] M. Ha, S. H. Kim, H. Kim, K. Kwon, N. Giang, and D. Kim, "Snail gateway: Dual-mode wireless access points for wifi and ip-based wireless sensor networks in the internet of things," in *Proc. IEEE Consum. Commun. Netw. Conf.* (CCNC), 2012, pp. 169–173.

[17] X. Xie, D. Deng, and X. Deng, "Design of embedded gateway software framework for heterogeneous networks interconnection," in *Proc. Int. Conf. Electron. Optoelectron.* (ICEOE), 2011.

[18] Digi-key corporation's website [Online]. Available: http://www.digikey.com/product-detail/en/CC2531F256RHAT/296-25186-2-ND/2171344?WT.mc_id=PLA_2171344

[19] (2013). Insteon compared. White Paper [Online]. Available: https://www.insteon.com/pdf/insteoncompared.pdf

[20] C. Corporation. (2005). Wi-fi radio characteristics and the cost of wlan implementation [Online]. Available: http://www.connect802.com/download/techpubs/2005/commercial_radios_E0523-15.pdf

[21] H.-C. Hsieh and C.-H. Lai, "Internet of things architecture based on integrated plc and 3g communication networks," in *Proc. IEEE Int. Conf. Parallel Distrib. Syst.*, 2011, pp. 853–856.

[22] Z. Shi, K. Liao, S. Yin, and Q. Ou, "Design and implementation of the mobile internet of things based on TD-SCDMA network," in *Proc. IEEE Int. Conf. Inf. Theory Inf. Secur.*, 2010, pp. 954–957.

[23] J.-M. Liang, J.-J. Chen, H.-H. Cheng, and Y.-C. Tseng, "An energy-efficient sleep scheduling with QoS consideration in 3gpp LTE-advanced networks for internet of things," *IEEE J. Emerging Sel. Topics Circuits Syst.*, vol. 3, no. 1, pp. 13–22, Mar. 2013.

[24] B. Wang, Y. Wu, F. Han, Y.-H. Yang, and K. J. R. Liu, "Green wireless communications: A time-reversal paradigm," *IEEE J. Sel. Areas Commun.*, Special on Energy-Efficient Wireless Communications, vol. 29, no. 8, pp. 1698–1710, Sep. 2011.

[25] F. Han, Y.-H. Yang, B. Wang, Y. Wu, and K. J. R. Liu, "Time-reversal division multiple access over multi-path channels," *IEEE Trans. Commun.*, vol. 60, no. 7, pp. 1953–1965, Jul. 2012.

[26] Y. Chen, Y. Yang, F. Han, and K. J. R. Liu, "Time-reversal wideband communications," *IEEE Signal Process. Lett.*, vol. 20, no. 12, pp. 1219–1222, Dec. 2013.

[27] Y.-H. Yang, B. Wang, W. S. Lin, and K. J. R. Liu, "Near-optimal waveform design for sum rate optimization in time-reversal multiuser downlink systems," *IEEE Trans. Wireless Commun.*, vol. 12, no. 1, pp. 346–357, Jan. 2013.

[28] B. Y. Zeldovich, N. F. Pilipetsky, and V. V. Shkunov, *Principles of Phase Conjugation.* Berlin, Germany: Springer-Verlag, 1985.

[29] A. P. Brysev, L. M. Krutyanskii, and V. L. Preobrazhenskii, "Wave phase conjugation of ultrasonic beams," *Phys.-Uspekhi*, vol. 41, no. 8, pp. 793–805, 1998.

[30] M. Fink, C. Prada, F. Wu, and D. Cassereau, "Self focusing in inhomogeneous media with time reversal acoustic mirrors," in *Proc. IEEE Ultrason. Symp.*, 1989, vol. 2, pp. 681–686.

[31] C. Prada, F. Wu, and M. Fink, "The iterative time reversal mirror: A solution to self-focusing in the pulse echo mode," *J. Acoust. Soc. Amer.*, vol. 90, no. 2, pp. 1119–1129, 1991.

[32] M. Fink, "Time reversal of ultrasonic fields. I. Basic principles," *IEEE Trans. Ultrason. Ferroelectr. Freq. Control*, vol. 39, no. 5, pp. 555–566, 1992.

[33] C. Dorme and M. Fink, "Focusing in transmit–receive mode through inhomogeneous media: The time reversal matched filter approach," *J. Acoust. Soc. Amer.*, vol. 98, no. 2, pp. 1155–1162, 1995.

[34] A. Derode, P. Roux, and M. Fink, "Robust acoustic time reversal with high-order multiple scattering," *Phys. Rev. Lett.*, vol. 75, pp. 4206–4209, Dec. 1995.

[35] W. A. Kuperman, W. S. Hodgkiss, H. C. Song, T. Akal, C. Ferla, and D. R. Jackson, "Phase conjugation in the ocean: Experimental demonstration of an acoustic time-reversal mirror," *J. Acoust. Soc. Amer.*, vol. 103, no. 1, pp. 25–40, 1998.

[36] H. C. Song, W. A. Kuperman, W. S. Hodgkiss, T. Akal, and C. Ferla, "Iterative time reversal in the ocean," *J. Acoust. Soc. Amer.*, vol. 105, no. 6, pp. 3176–3184, 1999.

[37] D. Rouseff, D. Jackson, W. L. J. Fox, C. Jones, J. Ritcey, and D. Dowling, "Underwater acoustic communication by passive-phase conjugation: Theory and experimental results," *IEEE J. Ocean. Eng.*, vol. 26, no. 4, pp. 821–831, Oct. 2001.

[38] G. Edelmann, T. Akal, W. Hodgkiss, S. Kim, W. Kuperman, and H. C. Song, "An initial demonstration of underwater acoustic communication using time reversal," *IEEE J. Ocean. Eng.*, vol. 27, no. 3, pp. 602–609, Jul. 2002.

[39] B. E. Henty and D. D. Stancil, "Multipath-enabled super-resolution for RF and microwave communication using phase-conjugate arrays," *Phys. Rev. Lett.*, vol. 93, p. 243904, Dec. 2004.

[40] G. Lerosey, J. de Rosny, A. Tourin, A. Derode, G. Montaldo, and M. Fink, "Time reversal of electromagnetic waves," *Phys. Rev. Lett.*, vol. 92, p. 193904, May 2004.

[41] R. C. Qiu, C. Zhou, N. Guo, and J. Q. Zhang, "Time reversal with MISO for ultrawideband communications: Experimental results," *IEEE Antennas Wireless Propag. Lett.*, vol. 5, no. 1, pp. 269–273, Dec. 2006.

[42] G. Lerosey, J. de Rosny, A. Tourin, A. Derode, G. Montaldo, and M. Fink, "Time reversal of electromagnetic waves and telecommunications," *Radio Sci.*, vol. 40, pp. 1–10, 2005.

[43] G. Lerosey, J. de Rosny, A. Tourin, A. Derode, and M. Fink, "Time reversal of wideband microwaves," *Appl. Phys. Lett.*, vol. 88, p. 154101, Apr. 2006.

[44] I. H. Naqvi, G. E. Zein, G. Lerosey, J. de Rosny, P. Besnier, A. Tourin, and M. Fink, "Experimental validation of time reversal ultrawide-band communication system for high data rates," *IET Microwaves Antennas Propag.*, vol. 4, pp. 643–650, 2010.

[45] J. de Rosny, G. Lerosey, and M. Fink, "Theory of electromagnetic time-reversal mirrors," *IEEE Trans. Antennas Propag.*, vol. 58, no. 10, pp. 3139–3149, Oct. 2010.

[46] M. Emami, M. Vu, J. Hansen, A. J. Paulraj, and G. Papanicolaou, "Matched filtering with rate back-off for low complexity communications in very large delay spread channels," in *Proc. Conf. Record 38th Asilomar Conf. Signals Syst. Comput.*, 2004, vol. 1, pp. 218–222.

[47] H. T. Nguyen, I. Z. Kovacs, and P. C. F. Eggers, "A time reversal transmission approach for multiuser UWB communications," *IEEE Trans. Antennas Propag.*, vol. 54, no. 11, pp. 3216–3224, Nov. 2006.

[48] N. Guo, B. M. Sadler, and R. C. Qiu, "Reduced-complexity uwb time-reversal techniques and experimental results," *IEEE Trans. Wireless Commun.*, vol. 6, no. 12, pp. 4221–4226, Dec. 2007.

[49] Y.-H. Yang and K. J. R. Liu, "Joint waveform design and interference pre-cancellation for time-reversal systems," *IEEE Trans. Commun.*, submitted.

[50] F. Han and K. J. R. Liu, "A multiuser TRDMA uplink system with 2D parallel interference cancellation," *IEEE Trans. Commun.*, to be published.

[51] P. Kyritsi and G. Papanicolaou, "One-bit time reversal for wlan applications," in *Proc. IEEE Int. Symp. Pers. Indoor Mobile Radio Commun.*, 2005, pp. 532–536.

[52] D.-T. Phan-Huy, S. B. Halima, and M. Helard, "Frequency division duplex time reversal," in *Proc. IEEE Globecom*, 2011, pp. 1–5.

[53] G. Lerosey, J. de Rosny, A. Tourin, and M. Fink, "Focusing beyond the diffraction limit with far-field time reversal," *Science*, vol. 315, pp. 1120–1122, Feb. 2007.

[54] F. Lemoult, G. Lerosey, J. de Rosny, and M. Fink, "Resonant metalenses for breaking the diffraction barrier," *Phys. Rev. Lett.*, vol. 104, p. 203901, May 2010.

[55] R. C. Qiu, C. Zhou, N. Guo, and J. Q. Zhang, "Time reversal with MISO for ultra-wideband communications: Experimental results," *IEEE Antenna Wireless Propag. Lett.*, vol. 5, no. 1, pp. 269–273, Dec. 2006.

[56] K. F. Sander and G. A. L. Reed, in *Transmission and Propagation of Electromagnetic Waves*, 2nd ed. New York, NY, USA: Cambridge Univ. Press, 1986.

[57] J. M. F. Moura and Y. Jin, "Time reversal imaging by adaptive interference canceling," *IEEE Trans. Signal Process.*, vol. 56, no. 1, pp. 233–247, Jan. 2008.

[58] J. M. F. Moura and Y. Jin, "Detection by time reversal: Single antenna," *IEEE Trans. Signal Process.*, vol. 55, no. 1, pp. 187–201, Jan. 2007.

[59] Y. Jin and J. M. F. Moura, "Time-reversal detection using antenna arrays," *IEEE Trans. Signal Process.*, vol. 57, no. 4, pp. 1396–1414, Apr. 2009.

[60] F. Han, Y.-H. Yang, B. Wang, Y. Wu, and K. J. R. Liu, "Time-reversal division multiple access in multi-path channels," in *Proc. Global Telecommun. Conf.*, 2011, pp. 1–5.

[61] M. Lienard, P. Degauque, V. Degardin, and I. Vin, "Focusing gain model of time-reversed signals in dense multipath channels," *IEEE Antennas Wireless Propag. Lett.*, vol. 11, pp. 1064–1067, Aug. 2012.

[62] G. Montaldo, G. Lerosey, A. Derode, A. Tourin, J. de Rosny, and M. Fink, "Telecommunication in a disordered environment with iterative time reversal," *Waves Random Media*, vol. 14, pp. 287–302, May 2004.

[63] F. Lemoult, G. Lerosey, J. de Rosny, and M. Fink, "Manipulating spatiotemporal degrees of freedom of waves in random media," *Phys. Rev. Lett.*, vol. 103, p. 173902, Oct. 2009.

[64] X. Zhou, P. Eggers, P. Kyritsi, J. Andersen, G. Pedersen, and J. Nilsen, "Spatial focusing and interference reduction using MISO time reversal in an indoor application," in *Proc. IEEE Workshop Statist. Signal Process.* (SSP), 2007, pp. 307–311.

[65] J. Proakis and M. Salehi, in *Digital Communications*, 5th ed. New York, NY, USA: McGraw-Hill, 2008.

[66] F. Rashid-Farrokhi, K. J. R. Liu, and L. Tassiulas, "Transmit beamforming and power control for cellular wireless systems," *IEEE J. Sel. Areas Commun.*, vol. 16, no. 8, pp. 1437–1450, Oct. 1998.

[67] F. Rashid-Farrokhi, L. Tassiulas, and K. J. R. Liu, "Joint optimal power control and beamforming in wireless networks using antenna arrays," *IEEE Trans. Commun.*, vol. 46, no. 10, pp. 1313–1324, Oct. 1998.

[68] Y.-H. Yang, S.-C. Lin, and H.-J. Su, "Multiuser MIMO downlink beamforming based on group maximum SINR filtering," *IEEE Trans. Signal Process.*, vol. 59, no. 4, pp. 1746–1758, Apr. 2011.

[69] H. Sampath, P. Stoica, and A. Paulraj, "Generalized linear precoder and decoder design for MIMO channels using the weighted MMSE criterion," *IEEE Trans. Commun.*, vol. 49, no. 12, pp. 2198–2206, Dec. 2001.

[70] F. Dietrich, R. Hunger, M. Joham, and W. Utschick, "Linear precoding over time-varying channels in TDD systems," in *Proc. ICASSP'03*, 2003, vol. 5, pp. 117–120.

[71] Z. Ahmadian, M. Shenouda, and L. Lampe, "Design of pre-rake DS-UWB downlink with pre-equalization," *IEEE Trans. Commun.*, vol. 60, no. 2, pp. 400–410, Feb. 2012.

[72] Y. Jin, J. M. Moura, and N. O'Donoughue, "Adaptive time reversal beamforming in dense multipath communication networks," in *Proc. 42nd Asilomar Conf. Signals Syst. Comput.*, Oct. 2008, pp. 2027–2031.

[73] R. C. Daniels and R. W. Heath, "Improving on time-reversal with MISO precoding," in *Proc. 8th Int. Symp. Wireless Pers. Commun. Conf.*, Aalborg, Denmark, 2005.

[74] L.-U. Choi and R. D. Murch, "A transmit preprocessing technique for multiuser MIMO systems using a decomposition approach," *IEEE Trans. Wireless Commun.*, vol. 3, no. 1, pp. 2–24, Jan. 2004.

[75] P. Kyritsi, G. Papanicolaou, P. Eggers, and A. Oprea, "Time reversal techniques for wireless communications," in *Proc. IEEE Veh. Technol. Conf.*, 2004, vol. 4, pp. 47–51.

[76] M. Brandt-Pearce, "Transmitter-based multiuser interference rejection for the downlink of a wireless CDMA system in a multipath environment," *IEEE J. Sel. Areas Commun.*, vol. 18, no. 3, pp. 407–417, Mar. 2000.

[77] P. Kyritsi, P. Stoica, G. Papanicolaou, P. Eggers, and A. Oprea, "Time reversal and zero-forcing equalization for fixed wireless access channels," in *Proc. 39th Asilomar Conf. Signals Syst. Comput.*, 2005, pp. 1297–1301.

[78] C. Windpassinger, R. F. H. Fischer, T. Vencel, and J. Huber, "Precoding in multiantenna and multiuser communications," *IEEE Trans. Wireless Commun.*, vol. 3, no. 4, pp. 1305–1316, Jul. 2004.

[79] W. Yu, D. Varodayan, and J. Cioffi, "Trellis and convolutional precoding for transmitter-based interference presubtraction," *IEEE Trans. Commun.*, vol. 53, no. 7, pp. 1220–1230, Jul. 2005.

[80] M. H. M. Costa, "Writing on dirty paper," *IEEE Trans. Inf. Theory*, vol. 29, no. 3, pp. 439–441, May 1983.

[81] Media access control [Online]. Available: http://en.wikipedia.org/wiki/Media_access_control

[82] G. Bianchi, "Performance analysis of the ieee 802.11 distributed coordination function," *IEEE J. Sel. Areas Commun.*, vol. 18, no. 3, pp. 535–547, Mar. 2000.

[83] M. Ergen, Ieee 802.11 tutorial [Online]. Available: http://wow.eecs.berkeley.edu/ergen/docs/ieee.pdf

[84] Even Steve Jobs has demo hiccups [Online]. Available: http://news.cnet.com/8301-31021_3-20007009-260.html

[85] A/D Converters, Texas Instrument 2013. [Online]. Available: http://www.ti.com/lsds/ti/data-converters/analog-to-digital-converter-products.page/.

[86] A. Kohlenberg, "Exact interpolation of band-limited functions," *J. Appl. Phys.*, vol. 24, no. 12, pp. 1432–1436, 1953.

[87] Y.-P. Lin and P. Vaidyanathan, "Periodically nonuniform sampling of bandpass signals," *IEEE Trans. Circuits Syst. II: Analog Digital Signal Process.*, vol. 45, no. 3, pp. 340–351, Mar. 1998.

[88] M. El-Chammas and B. Murmann, "General analysis on the impact of phase-skew in time-interleaved ADCs," *IEEE Trans. Circuits Syst. I: Regular Papers*, vol. 56, no. 5, pp. 902–910, May 2009.

[89] P. Nikaeen and B. Murmann, "Digital compensation of dynamic acquisition errors at the front-end of high-performance a/d converters," *IEEE J. Sel. Topics Signal Process.*, vol. 3, no. 3, pp. 499–508, Jun. 2009.

[90] Y. Eldar and A. Oppenheim, "Filterbank reconstruction of bandlimited signals from nonuniform and generalized samples," *IEEE Trans. Signal Process.*, vol. 48, no. 10, pp. 2864–2875, Oct. 2000.

[91] Y. Tian, D. Zeng, and T. Zeng, "Design and implementation of multifrequency front end using bandpass over sampling," in *Proc. IET Int. Radar Conf.*, 2009, pp. 1–4.

[92] J. Tropp, J. Laska, M. Duarte, J. Romberg, and R. Baraniuk, "Beyond nyquist: Efficient sampling of sparse bandlimited signals," *IEEE Trans. Inf. Theory*, vol. 56, no. 1, pp. 520–544, Jan. 2010.

[93] M. Mishali and Y. Eldar, "From theory to practice: Sub-nyquist sampling of sparse wideband analog signals," *IEEE J. Sel. Topics Signal Process.*, vol. 4, no. 2, pp. 375–391, Apr. 2010.
[94] "5g wiki," [Online]. Available: http://en.wikipedia.org/wiki/5G.

Yan Chen (S'06–M'11) received the Bachelor's degree from the University of Science and Technology of China, Hefei, China, in 2004, the M.Phil. degree from Hong Kong University of Science and Technology (HKUST), Hong Kong, China, in 2007, and the Ph.D. degree from the University of Maryland, College Park, MD, USA, in 2011.

His current research interests include data science, network science, game theory, social learning and networking, as well as signal processing and wireless communications.

Dr. Chen is the recipient of multiple honors and awards including best paper award from IEEE GLOBECOM, in 2013, Future Faculty Fellowship and Distinguished Dissertation Fellowship Honorable Mention from the Department of Electrical and Computer Engineering, in 2010 and 2011, respectively, Finalist of Deans Doctoral Research Award from A. James Clark School of Engineering, University of Maryland, in 2011, and Chinese Government Award for outstanding students abroad, in 2011.

Feng Han (S'08–M'14) received the B.S. and M.S. degrees from Tsinghua University, Beijing, China, in 2007 and 2009, respectively, and the Ph.D. degree from the University of Maryland, College Park, MD, USA, in 2013, all in electrical engineering.

Currently, he is a Senior Engineer with Corporate Research and Development, Qualcomm Inc., San Diego, CA, USA. His research interests include wireless communications and networking, game theory, signal processing, and communication theory.

He is a recipient of the First Prize in the 19th Chinese Mathematical Olympiad, the Best Thesis Award of Tsinghua University, the honor of Excellent Graduate of Tsinghua University, the A. James Clark School of Engineering Distinguished Graduate Fellowship, in 2009, and the Future Faculty Fellowship, in 2012, both from the University of Maryland. His work on time reversal technique was recognized by the university-level Invention of the Year Award and The Jimmy H. C. Lin Invention Award, both at the University of Maryland, in 2013, and his work on MIMO system received a Best Paper Award for at IEEE WCNC'08.

Yu-Han Yang (S'06) received the B.S. degree in electrical engineering, in 2004, the M.S. degree in computer science and communication engineering, in 2007, from National Taiwan University, Taipei, Taiwan, and the Ph.D. degree in electrical and computer engineering from the University of Maryland, College Park, MD, USA, in 2013.

His research interests include wireless communication and signal processing.

Dr. Yang received Class A Scholarship from the Department of Electrical and Computer Engineering (ECE), National Taiwan University, Taipei, Taiwan, in Fall 2005 and Spring 2006. He is a recipient of Study Abroad Scholarship from Taiwan (R.O.C.) government, in 2009–2010. He received the University of Maryland Innovation Award in 2013.

Hang Ma received the B.S. degree in information engineering from Northwestern Polytechnical University, Xi'an, China, in 2010. Currently, he is pursuing the Ph.D. degree at the University of Maryland, College Park, MD, USA.

His research interests include wireless communication and signal processing.

Mr. Ma received the honor of Outstanding Graduate of Northwestern Polytechnical University, in 2010.

Yi Han received the B.S. degree in electrical engineering from Zhejiang University, Hangzhou, China, in 2011. Currently, he is pursuing the Ph.D. degree from the Department of Electrical and Computer Engineering, University of Maryland, College Park, MD, USA.

His current research interests mainly focus on time-reversal communication technology.

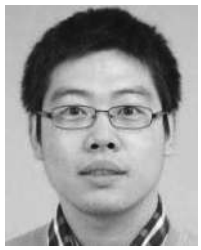

Chunxiao Jiang (S'09–M'13) received the B.S. degree in information engineering from Beijing University of Aeronautics and Astronautics (Beihang University), Beijing, China, in 2008 and the Ph.D. degree from Tsinghua University (THU), Beijing, China, in 2013, both with the highest honors.

Currently, he is a Post-Doctor in EE Department, THU, along with Prof. Yong Ren. He was a Research Associate in ECE Department of UMD with Prof. K. J. Ray Liu. From 2011 to 2012, he visited the Signals and Information Group (SIG), Department of Electrical and Computer Engineering (ECE), University of Maryland (UMD), College Park, MD, USA, supported by China Scholarship Council (CSC) for 1 year. His research interests include the applications of game theory and queuing theory in wireless communication and networking and social networks.

Dr. Jiang received the Best Paper Award from IEEE GLOBECOM, in 2013, the Beijing Distinguished Graduated Student Award, Chinese National Fellowship and Tsinghua Outstanding Distinguished Doctoral Dissertation, in 2013.

Hung-Quoc Lai (M'11) received the B.S. (cum laude), M.S., and Ph.D. degrees from the University of Maryland, College Park, MD, USA, in 2004, 2006, and 2011, respectively, all in electrical engineering.

His research interests include ultrawideband communications, cooperative communications, and networking.

Dr. Lai is a Gates Millennium Scholar. He is the recipient of university-level Distinguished Teaching Assistant Award from the University of Maryland and the 2005 George Corcoran Award from the Department of Electrical and Computer Engineering, University of Maryland.

David Claffey received the B.A. degree in physics from Cornell University, Ithaca, NY, USA, in 1985.

Zoltan Safar received the University Diploma in electrical engineering from the Technical University of Budapest, Budapest, Hungary, in 1996, and the M.S. and Ph.D. degrees in electrical and computer engineering from the University of Maryland, College Park, MD, USA, in 2001 and 2003, respectively.

After graduation, he was an Assistant Professor with the Department of Innovation, IT University of Copenhagen, Copenhagen, Denmark, until March 2005. Then, he joined Nokia, Copenhagen, Denmark, where he worked as a Senior Engineer on 3GPP Long Term Evolution (LTE) receiver algorithm design. From September 2007, he was a Senior Engineer with Samsung Electro-Mechanics, Atlanta, GA, USA, developing physical-layer signal processing algorithms for next-generation wireless communication systems. In February 2010, he became a Senior Software Engineer with Bloomberg L.P., NY, USA, and he designed and implemented software systems for monitoring, configuration and maintenance of the company's private communication network. Since October 2010, he has been with the Department of Electrical and Computer Engineering, University of Maryland, where he is the Director of the MS in Telecommunications program.His research interests include wireless communications and statistical signal processing, with particular focus on multi-antenna wireless communication systems, OFDM, and receiver algorithm design.

Dr. Safar received the Outstanding Systems Engineering Graduate Student Award from the Institute for Systems Research, University of Maryland, in 2003, and the Invention of the Year Award (together with W. Su and K. J. R. Liu) from the University of Maryland, in 2004.

K. J. Ray Liu (F'03) was a Distinguished Scholar-Teacher with the University of Maryland, College Park, MD, USA, in 2007, where he is a Christine Kim Eminent Professor of Information Technology. He leads the Maryland Signals and Information Group conducting research encompassing broad areas of signal processing and communications with recent focus on cooperative and cognitive communications, social learning and network science, information forensics and security, and green information and communications technology.

Dr. Liu is the recipient of numerous honors and awards including IEEE Signal Processing Society Technical Achievement Award and Distinguished Lecturer. He also received various teaching and research recognitions from the University of Maryland including university-level Invention of the Year Award; and Poole and Kent Senior Faculty Teaching Award, Outstanding Faculty Research Award, and Outstanding Faculty Service Award, all from A. James Clark School of Engineering. An ISI Highly Cited Author, he is a Fellow of AAAS. He is a Past President of IEEE Signal Processing Society, where he has served as Vice President—Publications and Board of Governor. He was the Editor-in-Chief of IEEE SIGNAL PROCESSING MAGAZINE and the founding Editor-in-Chief of *EURASIP Journal on Advances in Signal Processing*.